



Theoretical studies of conformational analysis and intramolecular dynamic phenomena

Ibon Alkorta¹ · José Elguero¹

Received: 21 March 2019 / Accepted: 3 June 2019 / Published online: 6 September 2019
© Springer Science+Business Media, LLC, part of Springer Nature 2019

Abstract

This review reports our computational studies of a variety of topics related to conformational analyses and intramolecular dynamic phenomena. Single and double bonds, open and ring systems, and chiral molecules devoid of chiral centers (atropisomers, propellers, scorpionates, helicenes, truxenes) will be reported. Studies that followed our contributions and that are related to them will also be cited. Some curious aspects such as the absence of influence of static fields on absolute chirality, the extension of CIP rules to supramolecular systems, libration of phenyl groups, and the barrier of 1,16-dehydro[6]helicene will be discussed.

Keywords Atranés · Atropisomerism · Carbohydrates · Chirality · Helicenes · Propellers · Scorpionates

Introduction

We have been interested in a series of topics that we will illustrate by a pair of references: (i) heterocycles, mainly azoles, and often related to their aromaticity [1, 2]; (ii) tautomerism, mainly of heterocyclic compounds [3, 4]; (iii) weak interactions [5, 6]; NMR properties, both chemical shifts [7, 8] and coupling constants [9, 10]; and (iv) crystallography [11, 12]. We will report in this review our results concerning conformational analysis and intramolecular dynamic phenomena, thus excluding intermolecular proton transfers [2, 13]. Obviously, some of these topics overlap.

We have followed Eliel and Wilen book plan [14] with small adaptations to include most of our contributions:

1. Stereochemistry of alkenes and aza analogs

- 1.1. CC double bonds
- 1.2. CN double bonds
- 1.3. NN double bonds

2. Conformation of acyclic molecules

- 2.1. CC and CN bonds

- 2.1.1. sp^3/sp^3
- 2.1.2. sp^3/sp^2
- 2.1.3. sp^2/sp^2
- 2.2. Amines, phosphines, and sulfur compounds
- 2.3. Atranés
3. Configuration and conformation of cyclic molecules
 - 3.1. Six-membered rings
 - 3.1.1. Carbohydrates
 - 3.1.2. Heterorings
 - 3.2. Other than six-membered rings
 - 3.2.1. Three-membered rings
 - 3.2.2. Four-membered rings
 - 3.2.3. Five-membered rings
 - 3.2.4. Rings larger than six-membered
 - 3.3. Stereochemistry of other related systems
4. Chirality in molecules devoid of chiral centers
 - 4.1. Biphenyls, atropisomerism
 - 4.2. Molecular propellers
 - 4.2.1. Methanes
 - 4.2.2. Borates (scorpionates)
 - 4.3. Helicenes
 - 4.4. Truxenes

✉ José Elguero
iqmbe17@iqm.csic.es

¹ Instituto de Química Médica, CSIC, Juan de la Cierva, 3,
E-28006 Madrid, Spain

The selection of these topics is based on our interests in dynamic phenomena but also in those of our coauthors that often wanted to know if theoretical calculations could provide a solid foundation to their experimental observations. Among them are Curt Wentrup (Australia), Artur M. S. Silva (Portugal), Rosa M. Claramunt (Spain), Krzysztof Zborowski (Poland), Patricio F. Provasi (Argentina), Juan Jesús López (Spain), Wolfgang Holzer (Austria), Janet E. Del Bene (USA), José Luis Serrano (Spain), Manuel Yáñez (Spain), Christian Roussel (France), Emilio J. Cocinero (Spain), and others. In this review covering our work from 1989 to 2019, our results will be discussed in rapport with literature results, in general subsequent to our work.

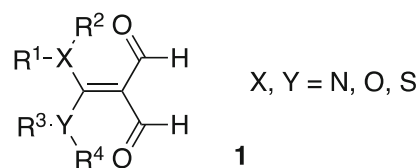
Stereochemistry of alkenes and aza analogs

CC double bonds

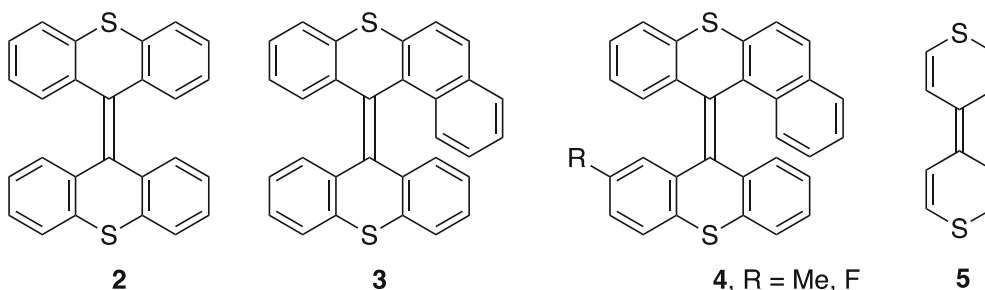
The rotational barriers about CC single, double, and triple bonds were studied at the B3LYP/6-311++G(d,p) level [[15]]. Intuitively, one expects that the barrier around a C≡C bond should be higher than that around a C=C bond, but that barrier is not physically observable. The conclusion was the rotational barrier around a CC triple bond could be estimated to be 355 kJ mol⁻¹ (leading to a double bond) or 645 kJ mol⁻¹

(leading to a single bond). These calculations were compared with the Cr–Cr quintuple bond [16].

Rotation around the π-C=C double bond, leaving the σ-(C=C) bond intact, is one of the most fundamental processes in chemistry. In the case of the central C=C bond in push-pull ethylenes **1** with R substituents like COR, CO₂R, NO₂, CN, The orthogonal state is not a biradical but a zwitterion [17]. The conformation and barriers of these compounds are determined by the presence (barriers of ~ 125 kJ mol⁻¹) or absence (barriers of ~55 kJ mol⁻¹) of intramolecular hydrogen bonds (IMHBs). For comparison purposes, the ethylene barrier amounts to 272 kJ mol⁻¹. The energy profiles in function of the dihedral angle θ follow an empirical equation related to the Pitzer equation for ethane [14]. For further related studies on this topic, see [18].



A further example of rotation about central CC bonds was studied in cases related to Feringa's molecular rotors [19].

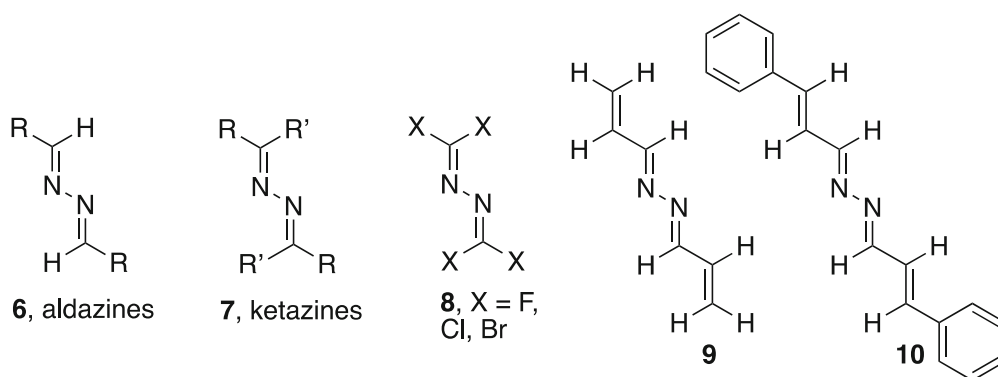


The isomerization barriers of bithioxanthenes **2–4** were calculated at the B3LYP/6-311++G(d,p) level; in the case of bis(4*H*-thiopyran) (**5**), a planar molecule, complete active space self-consistent field calculations (CASSCF) were carried out followed by Multi-State CASPT2 calculations on the singlet and triplet transition states [20]. The barriers for the singlet 90° were 106.0 (B3LYP/6-311++G(d,p)) and 92.6 kJ mol⁻¹ (CASPT2). Although there is a difference of 13.4 kJ mol⁻¹, the conclusion was that the excited states do not affect the energy barrier at low temperatures. Therefore, the barriers for the bithioxanthenes **2–4** were calculated at the B3LYP/6-311++G(d,p) level; these compounds present two conformations, one boat-like or up/up (**uu**) and the other chair-like or up/down (**ud**), the **ud** minima being more stable than the **uu** ones by about 34 kJ mol⁻¹. Their isomerization mechanisms,

inversion and rotation, have been studied; the rotation mechanism is always preferred.

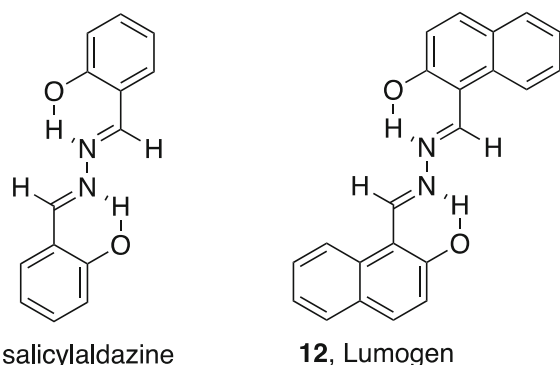
CN double bonds

The C=N group is presented in a variety of structures comprising imines, hydrazones, azines, and oximes. Although we have devoted a paper to hydrazones [21], our main interest was on azines. This is due that we studied experimentally these compounds several years ago [22–24] (for a recent review, see [25]). Two papers were devoted to computational studies of the structure of aldazines and ketazines, part 1 to simple compounds (**6**, **7**) [26] and part 2 to halogen (**8**) and α,β -unsaturated derivatives like **9** [27], including cinnamaldazine (**10**) [24].

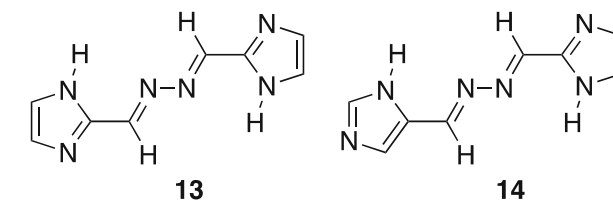


In the case of simple azines, B3LYP/6-311++G(d,p) calculations yield good geometries as well as *E/Z* ratios and IR spectra in agreement with experimental results; increasing the level of the calculations (MP2, QCISD) does not improve the geometries [26]. In the second paper, only B3LYP/6-311++G(d,p) calculations were carried out. For simple azines and for conjugated azines, *EE* and *EEEE* conformations, respectively, were preferred. Two mechanism of isomerization of CN double bonds, inversion and rotation, were studied for simple imines; in the case of azines, the TS has a “inversion-rotation” structure corresponding to barriers between 50 and 100 kJ mol⁻¹. The potential surface of **8** (X = F) was calculated [27].

Two further papers explore the structure of aldazines bearing aromatic substituents (**6**, R = aryl or heteroaryl). In the first case, the existence of IMHBs in salicylaldazine (**11**) and Lumogen (**12**) stabilizes the *EE* dihydroxy isomers but in the case of **12**, the hydroxy-oxo tautomer was observed in solution by NMR [28].



The structure of aldazines derived from formyl-1*H*-imidazoles, **13** and **14**, some of them double-labeled with ¹⁵N, has been studied by NMR (solution and solid-state) and by X-ray crystallography [29]. Computational calculations at the B3LYP/6-311++G(d,p) level were used to determine the conformation about CC bonds and the configuration about C=N ones. Tautomerism and lone pair/lone pair repulsions determined the preferred structures.



Barriers about C=N bonds in aldimines, oximes, hydrazones, and azines have been computed at the B3LYP/6-311++G(d,p) and G3B3 levels [30]. Bond rotation and nitrogen inversion processes were compared (see Fig. 1) and in all cases the inversion process is preferred save in the case of azines where there is some rotation character. These results were cited in a paper about the photochemistry of imines [31].

NN double bonds

Somewhat related to azines **13** and **14**, the structure of the azo derivative, 3(5),3'(5')-azopyrazole (**15**) was studied theoretically [32] because the *syn/anti* isomerization of azobenzene is the main strategy for modifying the distances in molecular machines [32] and references therein]. Energy calculations, ¹³C and ¹⁵N chemical shifts, ¹H–¹H coupling constants, and

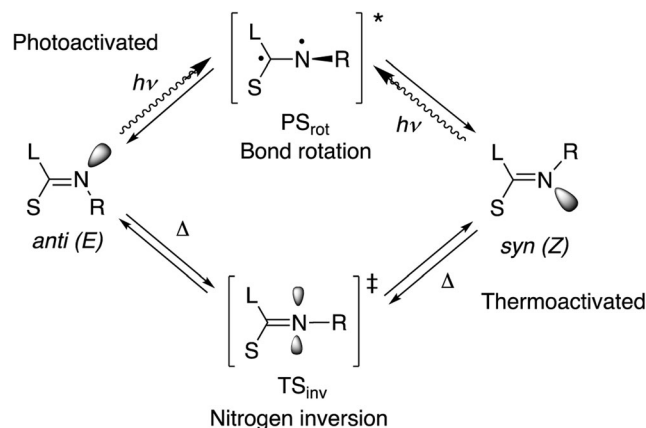
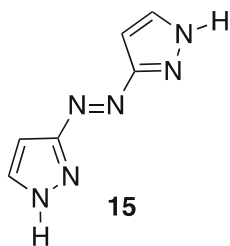


Fig. 1 Schematic representation of the rotation and inversion processes in imines

electronic spectra reduced the 20 possible calculated structures to only one, the 3,3'-Z,Z-anti-azopyrazole.



Conformation of acyclic molecules

CC and CN bonds

sp^3/sp^3

Interested in the relationships between molecular and supramolecular chemistry (for instance, extending the Cahn-Ingold-Prelog rules to supramolecular structures [33, 34]), we studied the rotational barriers about covalent bonds and hydrogen bonds, in particular, comparing 1,1,1-trifluoroethane (Csp^3-Csp^3 bond) with the trifluoromethane/ammonia complex (HB) [35]. These studies were extended to the extremely rare ${}^3J_{HH}$ bonds through two heteroatoms (H-N-N-H and H-N-O-H) [36–38] that were compared to the ${}^4J_{HH}$ in supramolecular complexes such as $[H_3N\cdots H\cdots NH_3]^+$, $[HOH\cdots NH_3]$ and $[HOH\cdots OH_2]$ [39]. Finally, the Karplus relationship was calculated for $H_3C-(C\equiv C)_n-CH_3$ systems in function of the number of CC triple bonds until $n = 6$; by extrapolation, it was estimated that for $n = 25$, the J_{HH} will amount to 0.1 Hz [40]. These studies have been extended by

other authors to ${}^3J_{HSi}$ spin–spin coupling constants [41] and to $F-(C\equiv C)_n-F$ J_{FF} coupling constants until $n = 11$ [42].

The conformations of other systems where two heteroatoms form the pivotal bond have also been studied. The most reported are X–O–O–Y related to oxygen peroxide (X = Y = H): racemization process and optical rotatory power (X = H, Y = CCH, CH_3 , CF_3 , *t*-Bu, CN, F, Cl) [43]; chiral discrimination in the hydrogen bonded dimers of X–O–O–H (X = H, CH_3 , CF_3 , HCO) [44]; resolution of the optical rotatory power into atomic contributions (X = H, Y = CH_3) [45, 46]; NMR of homo- and heterochiral complexes of X–O–O–Y with lithium cation (X, Y = H, CH_3) [47, 48]. The central atoms of the X–O–O–Y molecule have been replaced by S and Se and their hydrogen and chalcogen bonds studied [49]. Related to hydrazine are the $X_2-P-P-Y_2$ molecules, H_2P-PH_2 and H_2P-PHF ; their energy profiles on the rotation about the PP bond have been computed at the MP2/aug'-cc-pVTZ [50].

Somewhat related to this topic was the exploration of the methane surface [51]. Seven stationary points of the methane hypersurface were first explored concerning geometries and energies to check previous data. On these geometries, absolute 1H and ${}^{13}C$ NMR shieldings as well as ${}^1J_{CH}$ and ${}^2J_{HH}$ coupling constants were calculated. For planar methane, D_{4h} , the relative energies were 604 (CCD/6-311++G(d,p)), 575 (CCSD(T)/aug-cc-pVTZ), and 558 kJ mol^{-1} (M05-2X/aug-cc-pVTZ). Jackowski and Makulski reported these results in their work towards a ${}^{13}C$ scale for MAS NMR spectroscopy [52].

sp^3/sp^2

Concerning Csp^2-Csp^3 single bonds, the libration (restricted rotation) of phenyl groups in 2-benzyl-1H-benzimidazole (**16**) was determined by solid-state NMR (SSNMR) variable

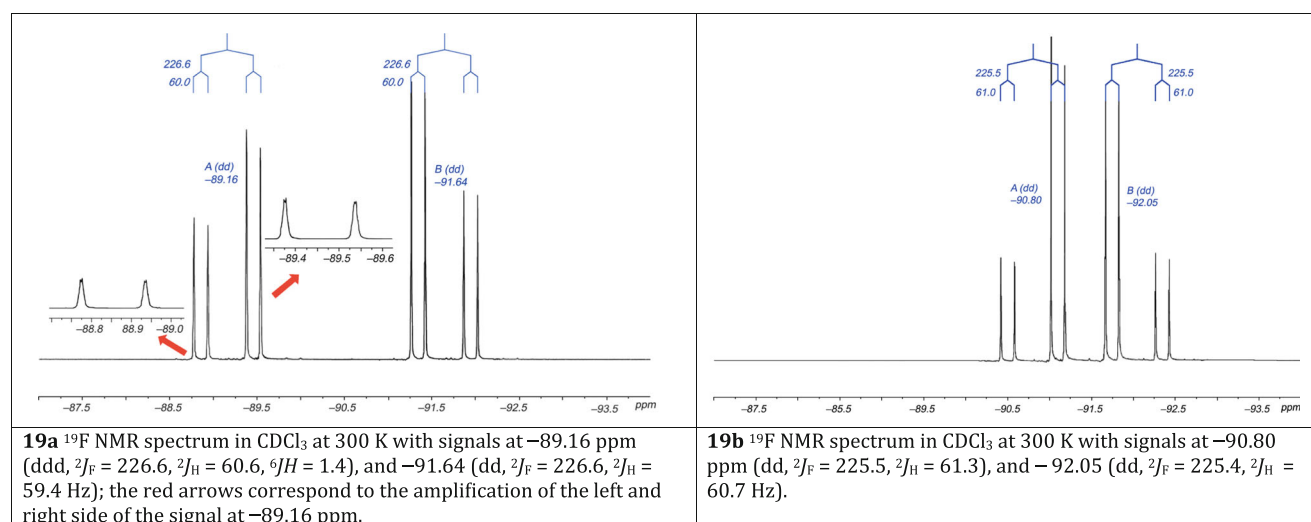
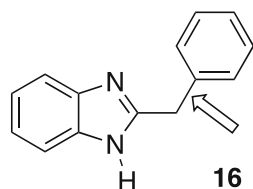


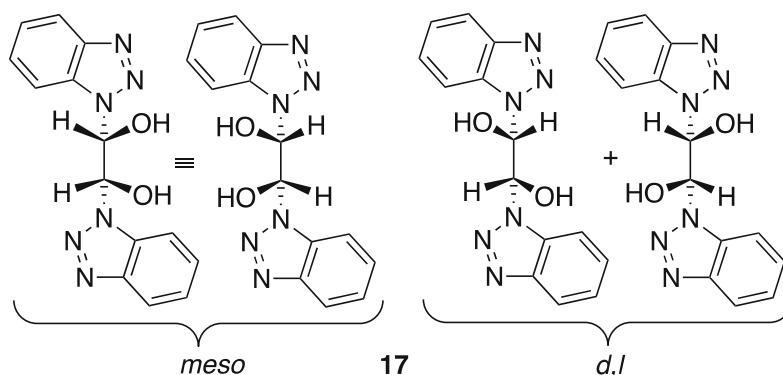
Fig. 2 The ${}^{19}F$ NMR spectra of compounds **19a** and **19b**

temperature experiments, although this phenomenon is not observed by X-ray crystallography. The barrier was calculated to be 59 kJ mol^{-1} , a rather high value compared with the calculated value for the gas phase (10 kJ mol^{-1} , B3LYP/6-311++G(d,p)) [53].



Our interest in azoles and benzazoles has resulted in several conformational papers related to Nsp^2 (pyrrole-like)– Csp^3 bonds conformations. Compound **16** presents a very unexplained behavior in the solid state, being an achiral compound in solution (due to CC bonds free rotation) and a chiral compound in the solid state (conglomerate) where always the same enantiomer is present [54, 55].

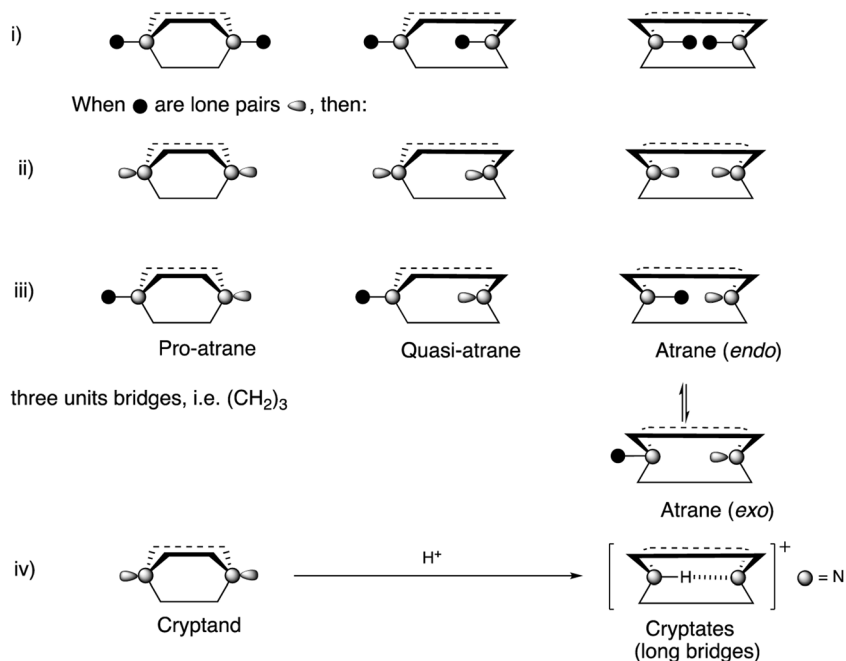
The double addition of azoles to glyoxal result in *meso* and *d,l* isomers like **17** in the case of 1*H*-benzotriazole [56]. Eight minimum energy conformations were calculated and compared with NMR results in solution in the case of pyrazole.

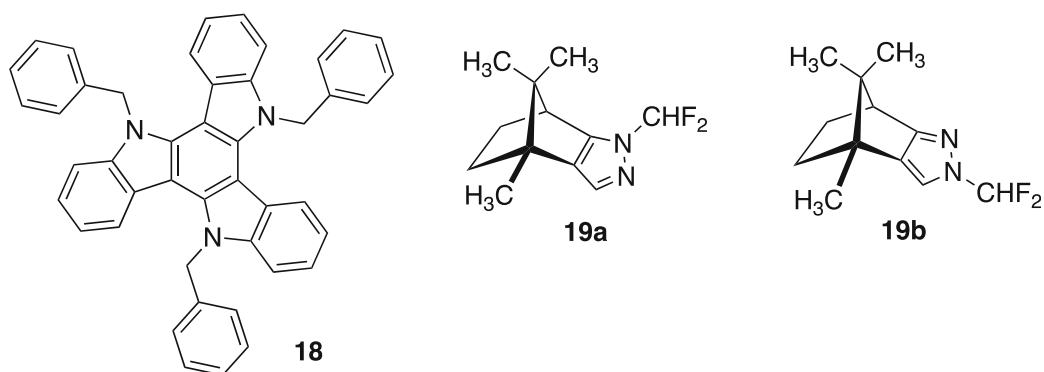


We have reported a series of studies of *N*-benzylazoles and *N*-benzylbenzazoles. The *N*-benzyl as well as other *N*-aryl and *N*-heteroaryl groups has clear conformational preferences and the CH_2 protons eventual anisochrony is very useful for

dynamic NMR studies (DNMR). Using this approach, the all-*syn* conformation of C_3 -symmetrical *N*-(Hetero)arylmethyl triindoles, for instance **18** in the case of benzyl, was ascertained [57].

Fig. 3 The structure of atranes (silatranes, phosphatranes, and related compounds)

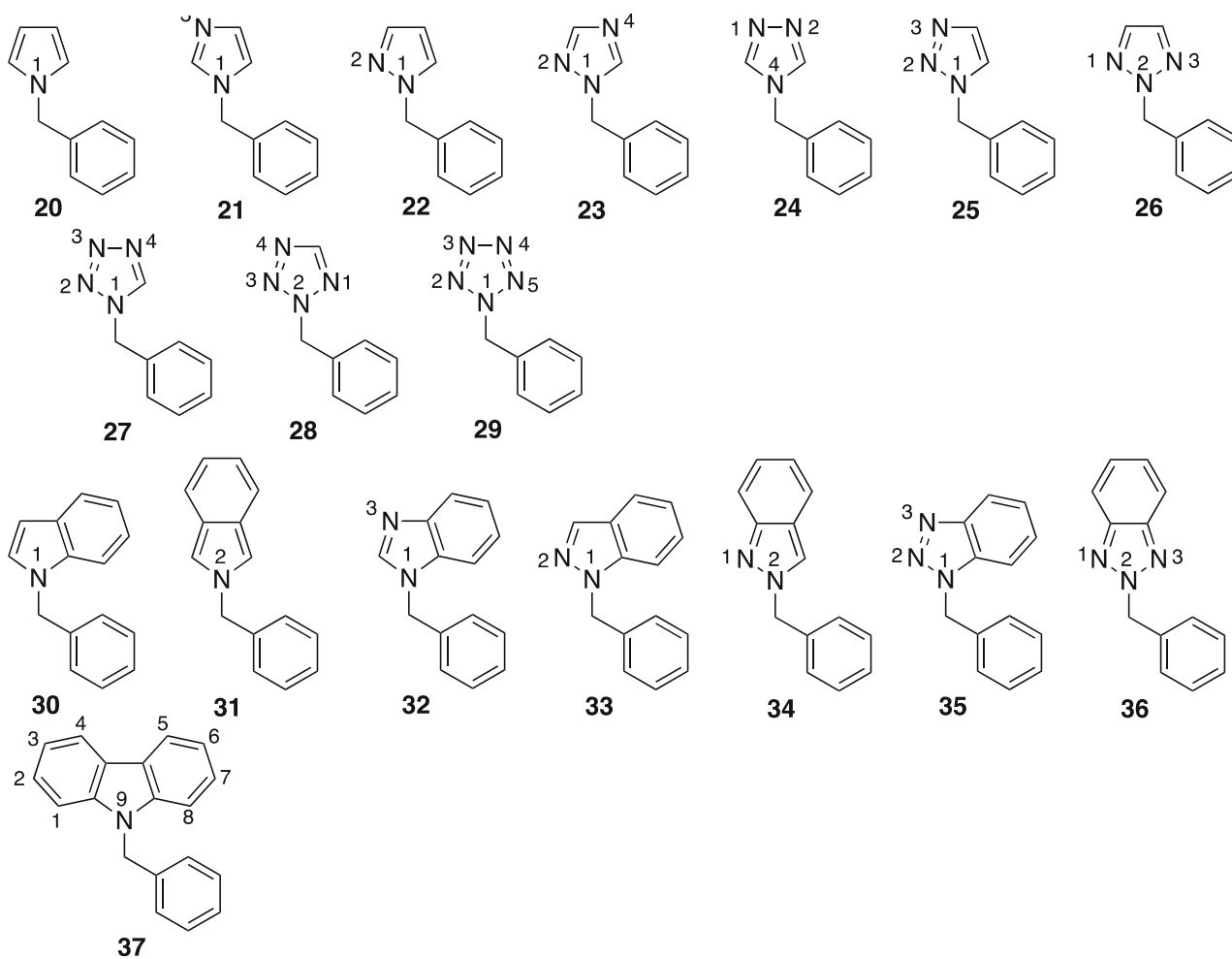




A group similar to the benzyl one but with fluorine instead of protons is the difluoromethyl that can be used as a chiral probe [58]; this group was never previously been studied. In the case of camphor derivatives **19a** and **19b**, the ^{19}F NMR spectra correspond to ABX systems of the diastereotopic fluorine atoms (Fig. 2).

A systematic experimental and theoretical study of the whole family of *N*-benzylazoles (**20–29**) and *N*-benzazoles

(**30–37**) was carried out and reported in two publications (compound **29** is unknown and compound **31** is very unstable, both were calculated) [59, 60]. Using a combination of X-ray crystallography, and NMR and DFT calculations, the structure and conformation, including rotational barriers of these compounds, were determined and the possibility to observe diastereotopic protons at very low temperatures discussed.



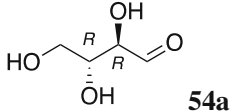
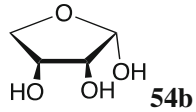
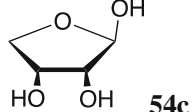
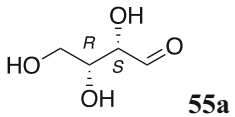
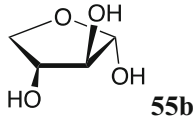
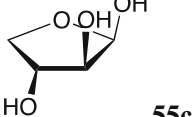
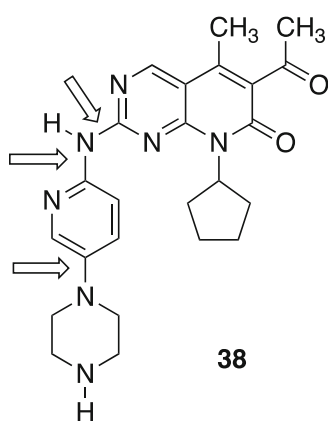
	Open-chain	α -furanose	β -furanose
D-erythrose (54)	 54a	 54b	 54c
D-threose (55)	 55a	 55b	 55c

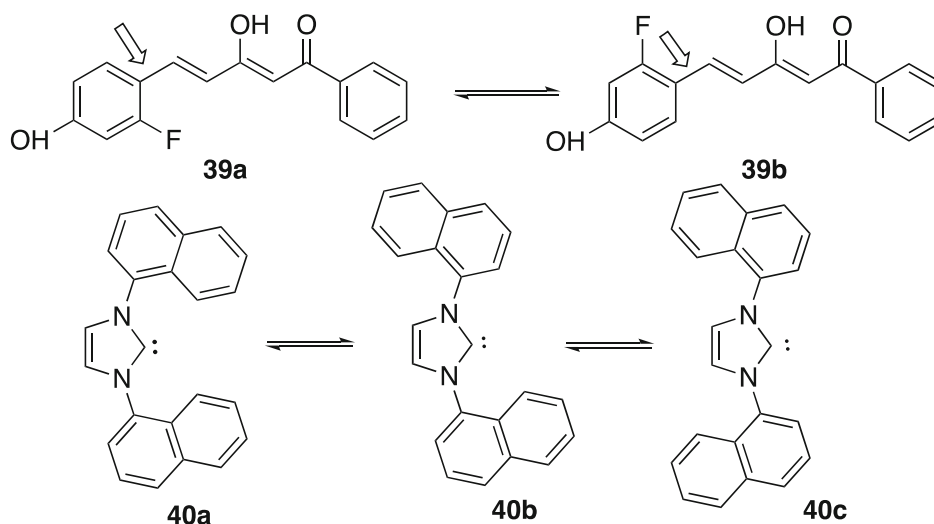
Fig. 4 Open-chain and α - and β -furanose configurations of D-erythrose (54) and D-threose (55)

One of the few papers concerning $Nsp^3-Csp^2(Ar)$ bonds reports the structure of palbociclib (38) [61] (for a review, see [62]).



sp^2/sp^2

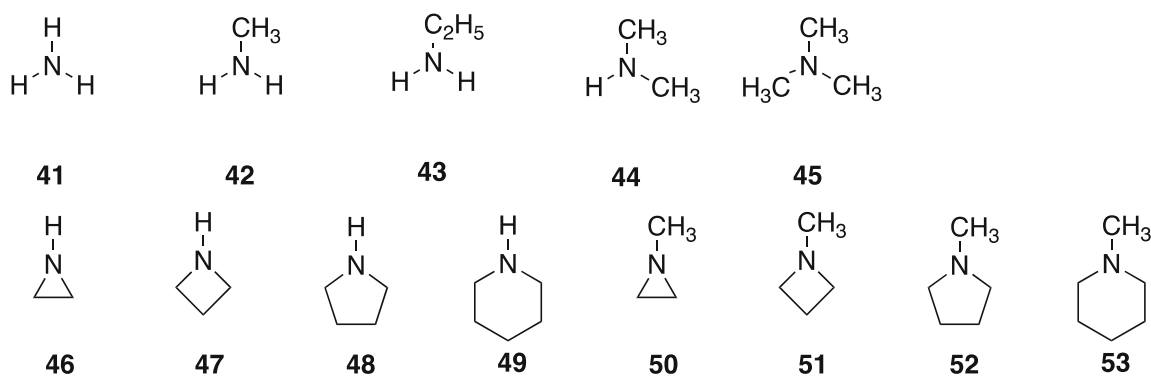
Some curcuminoids such as 39 present conformational structures related to rotation about single bonds linking two Csp^2 atoms [63], while the conformation of N -heterocyclic carbenes 40 (and related compounds) depends on the rotation about two $Nsp^2-Csp^2(Ar)$ bonds [64]. In this paper was introduced the use of a tesseract (hypercube) of 16 vertices and 32 edges representation that was used by other authors [65].



Amines, phosphines, and sulfur compounds

This topic is related to the previous one when the single bond involves an sp^3 nitrogen atom; for instance, carbenes 40 have

also been studied for imidazolines (no CC double bond) where the N atoms are clearly pyramidal [64]. The nitrogen inversion and its relevance in conformational analysis have been studied in 13 simple amines, 41 to 53, based on calculated chemical shifts [66].



The position of the N lone pair (LP) of a series of 17 amines and the 13 represented above plus azatetrahydane, azacubane, 1-azabicyclo[1.1.0]butane, and azirine has been located with the help of Bader's methodology; besides, a geometrical model based on symmetry was examined [67]. The related P inversion of phosphines was also studied [68–70].

The conformation of sulfamide itself, $\text{H}_2\text{N}-\text{SO}_2-\text{NH}_2$ [71], glibenclamide, a sulfamide derivative, $\text{R}-\text{HN}-\text{SO}_2-\text{Ar}$ [72], and rimonabant, a hydrazide [73], was also studied. These works have been cited several times [74–76].

Atranes

When the three legs of NR_3 or PR_3 are part of a cyclic system, the N inversion (amines) and the related P inversion (phosphines) results in the deformation of a basket (Fig. 3).

Two theoretical publications were devoted to the study of these compounds, the first one to the study of their

geometrical, energetic, and NMR properties [77], and the second one to the modulation of in:out and out:out conformations in $[\text{X}, \text{X}', \text{X}'']$ phosphatranes by Lewis acids [78]. This field is continuing to be very active [79, 80].

Configuration and conformation of cyclic molecules

Six-membered rings

Carbohydrates

This topic, part of the thesis of Luis Miguel Azofra, was not a usual topic of our research. In the case of D-erythrose (54) and D-threose (55), we characterized at the B3LYP/6-311++G(d,p) level 174 and 170 minima for the open-chain structures of 54 and 55, respectively. G3B3 calculations indicate that the α -

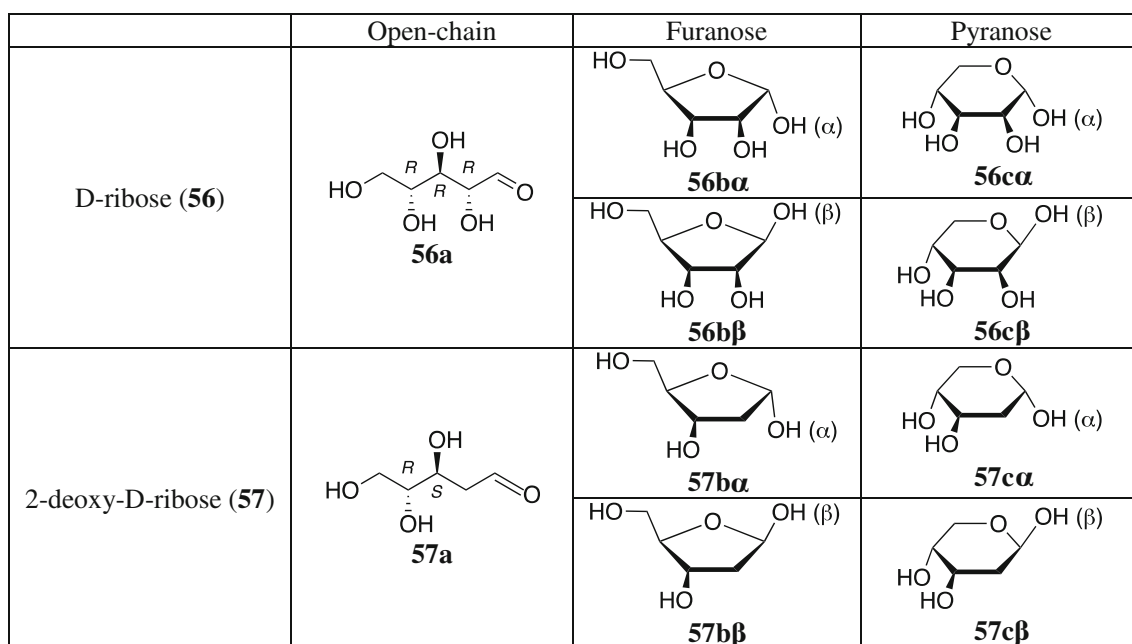


Fig. 5 Left to right and top to bottom: open-chain, furanose, and pyranose configurations of D-ribose and 2-deoxy-D-ribose. The orientation of the hydroxyl group on the anomeric carbon atom (C1) in the cyclic forms gives the α - (*exo* face) and β - (*endo* face) diastereoisomers.

Fig. 6 Triaziridine (**62**), minima (*uud* and *uuu*), and transition states (*udp*, *uup*, *ppp*)

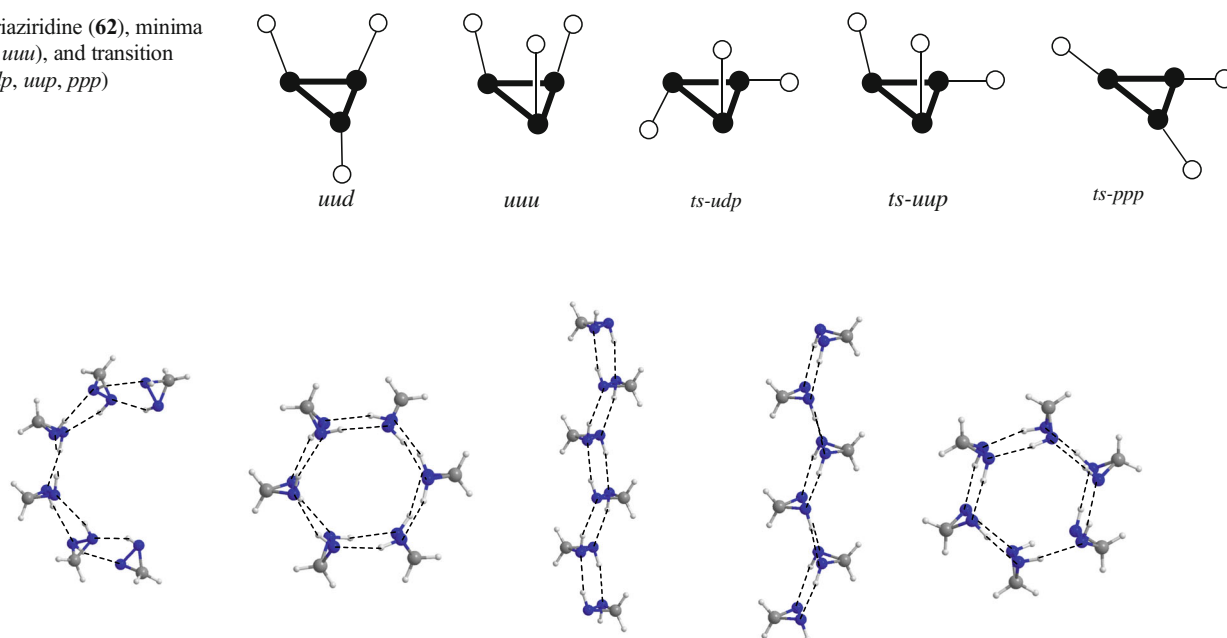


Fig. 7 Optimized geometries of the five configurations considered for the clusters. The ones shown correspond to the hexamer of **66**

furanose configuration is the most stable for both D-erythrose and D-threose. The hydrogen bonds present in these molecules were classified as 1-2, 1-3, or 1-4, based on the number of C–C bonds [81] (Fig. 4). In a subsequent paper, the acid catalysis of the mutarotation mechanism in the two aldotetroses, **54** and **55**, was studied at B3LYP/6-311++G(d,p) computational level in gas phase and in solution employing the PCM–water model. The acid catalysis has been studied taking into account the effect of (i) a classical Lewis acid as BH_3 , (ii) a classical hard-Pearson acid as Na^+ , (iii) two classical Brønsted acids such as H^+ and H_3O^+ , and (iv) the combined strategy using H_3O^+ and one bridge- H_2O molecule as an assistant in the proton transfer [82].

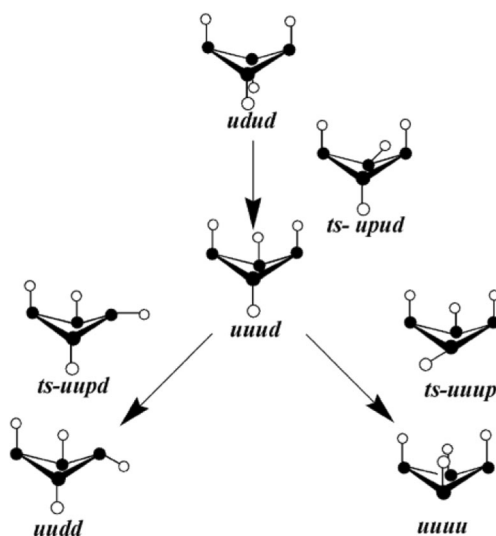


Fig. 8 Tetrazetidone **67** stationary points

The preceding works were followed by a study of D-ribose (**56**) and 2-deoxy-D-ribose (**57**) carbohydrates. A theoretical DFT (B3LYP and M06-2X) and MP2 study has been undertaken considering the five possible configurations (open-chain, α -furanose, β -furanose, α -pyranose, and β -pyranose) of these two carbohydrates with a comparison of the solvent treatment using only a continuum solvation model (PCM) and the PCM plus one explicit water molecule. In addition, experimental vibrational studies using both nonchiroptical (IR-Raman) and chiroptical (VCD) techniques have been carried out. The theoretical and experimental results show that α - and β -pyranose forms are the dominant configurations for both compounds (Fig. 5) [83]. This was followed by a full exploration of the conformational landscape of **56** and **57** monosaccharides in the gas phase which has been performed using DFT methods (B3LYP and M06-2X) [84]. Up to 954 and 668 stable structures have been obtained for D-ribose and 2-deoxy-D-ribose. For other authors' contribution to this field, see [85–92].

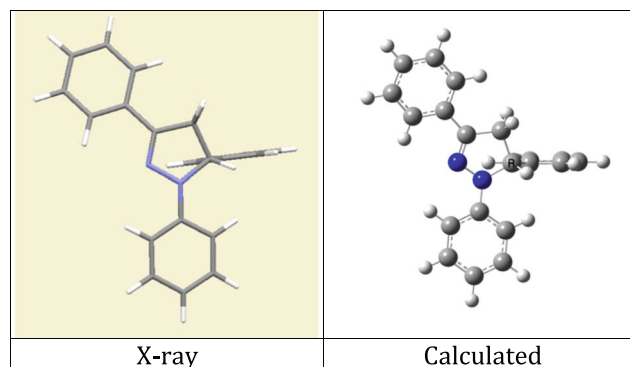


Fig. 9 Structures of compound **70**

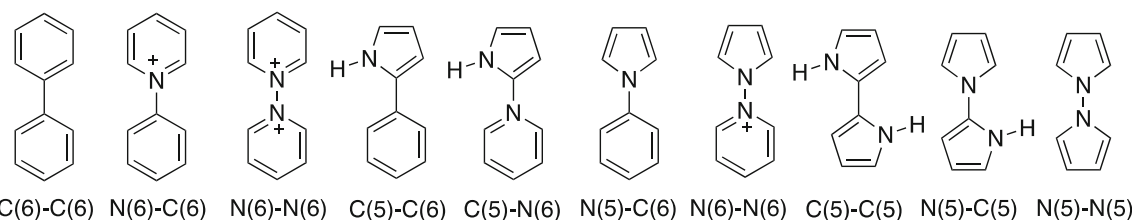
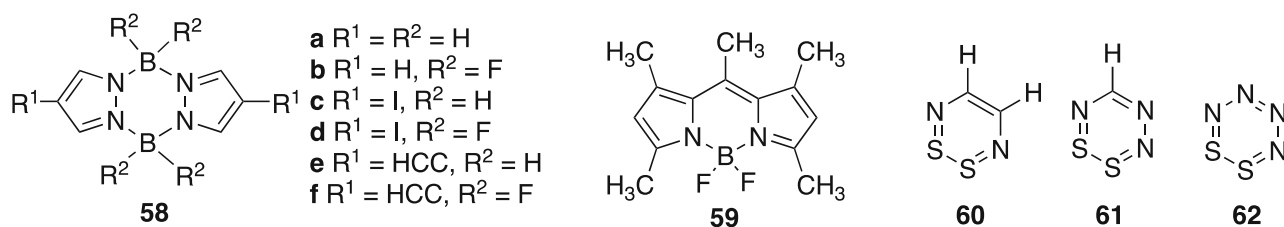


Fig. 10 6-6, 5-6, and 5-5 atropisomers. The C–Hs can be replaced by Ns and the N–Hs by Os or Ss

Heterorings

Some six-membered rings containing elements other than C, N, and O have been studied. Pyrazaboles **58a–58f** have four possible conformations, i.e., boat, chair, bent, and planar. The predominance of one of these conformations in the solid state (X-ray crystallography) depends on the R^1 and R^2 substitu-

ents. Theoretically (B3LYP/6-311+G** and MP2/6-31G* computational levels), the boat conformation is an energy minimum, with the planar and chair conformations as transition states in an energy diagram. In solution, the compounds are in a boat conformation (with a boat-to-boat dynamic equilibrium) irrespective of their crystal structures [93] (see also [94]).



- a** $R^1 = R^2 = H$
- b** $R^1 = H, R^2 = F$
- c** $R^1 = I, R^2 = H$
- d** $R^1 = I, R^2 = F$
- e** $R^1 = HCC, R^2 = H$
- f** $R^1 = HCC, R^2 = F$

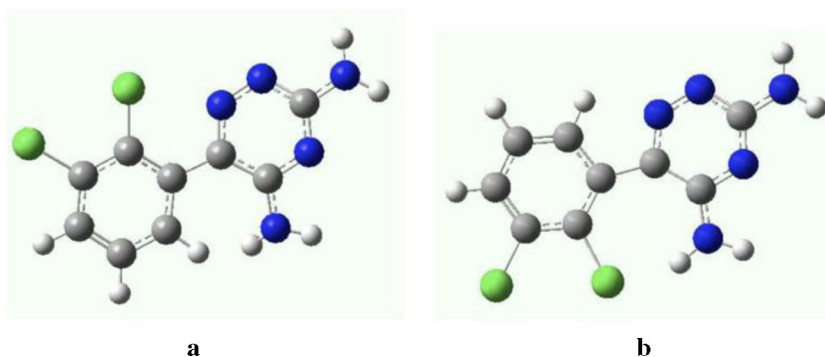
BODIPY 493/503 **59** is a pentamethyl derivative of the BODIPY skeleton [95]. Compound **59** is a bright, green fluorescent dye with similar excitation and emission to fluorescein with several uses in biochemistry, for staining lipids, membranes, and other lipophilic compounds. Its conformation was optimized at the B3LYP/6-311++G(d,p) computational level to afford a starting geometry for calculating NMR properties. Finally, three six-membered $-N=S-S=N-$ heterocycles **60–62**, all of them non-planar, have been studied theoretically [96].

Other than six-membered rings

Three-membered rings

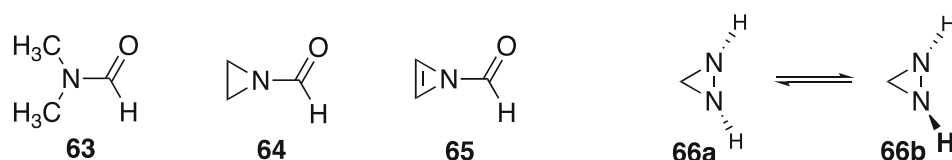
The conformational landscapes of triaziridine and the water trimer supramolecular system were calculated (Fig. 6) [B3LYP/6-311+G(3df,2p)] and compared; also the monofluoro and monochloro derivatives were calculated [97]. Both systems behave similarly; more importantly, even though in the former the energy required to induce conforma-

Fig. 11 a, b Structures of the two transition states of **88**



tional rearrangements is much smaller than that needed for typical molecular systems, there is a fairly good linear relationship between both magnitudes. Theoretical studies on triaziridine have been pursued at higher levels [98].

The rotation/inversion barriers of formamide (**63**), *N*-formyl aziridine (**64**), and *N*-formyl azirine (**65**) were calculated [MP2/6-311++G(d,p)]. The results provide a quantitative picture of the influence of ring strain on the properties of amides,



Diaziridine **66** has two conformations **a** (1*R*,2*S*) and **b** (1*S*,2*S*); the optical rotatory power of **66b** has been calculated (B3LYP/6-311++G(2d,2p) and MP2/6-311++G(d,p)) [102] as well as the barrier that separated **66a** of **66b** by a TS = 149.6 kJ mol⁻¹, conformer **b** being 25.1 kJ mol⁻¹ more stable than **a**. Five different topologies of the cluster that present two HB interactions per monomer have been considered (Fig. 7 shows the optimized ones for the hexamer). The preferred conformation **66b** is consistent with that of the 1,2,3-trisubstituted diaziridines [103].

The results show that the clusters with alternated chiral molecules are the preferred ones and that the proton transfer proceeds with low energetic barriers in the protonated systems. Proton transfer along the chains can invert stepwise the chirality of the molecules producing what we have called racemization waves [104].

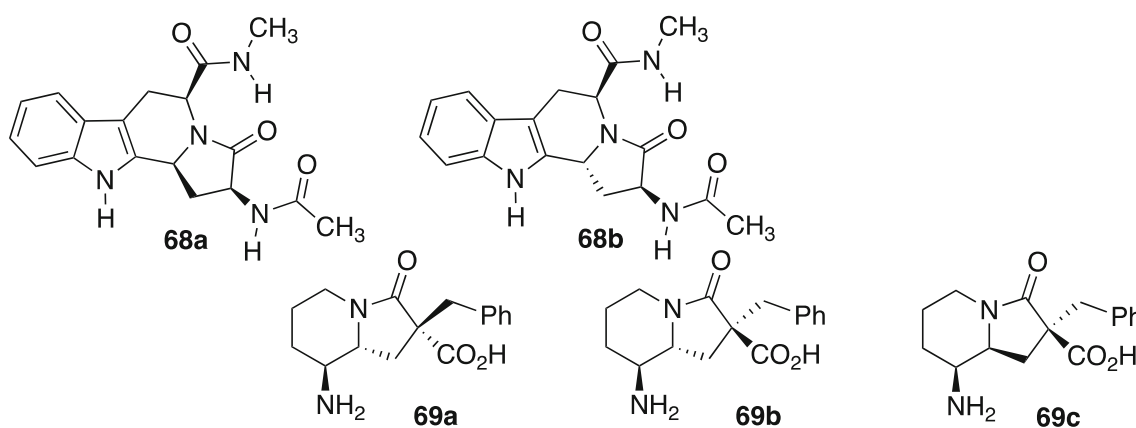
with special emphasis on the effects associated with nitrogen pyramidalization [99]. Related to this problem, the chemistry of bridged lactams has been reviewed [100] and the conformational aspects of cyclic peptides derived from aziridine-containing amino acids have been studied [101].

Four-membered rings

Similar studies than those reported previously on triaziridines and water trimers (section “Three-membered rings”) were carried out for tetrazetidine (**67**) (Fig. 8), water tetramers [97], and their monofluoro and monomethyl derivatives.

Five-membered rings

Molecular dynamics studies of 3-oxohexahydroindolizino[8,7-*b*]indole derivatives (**68**) were carried out in order to study their potential as novel β -turn mimetics [105, 106]. While **68a** and **68b** are able to adopt type II' β -turn conformations, in the case of **69a–69c**, they show extended conformations of non-standard folding.



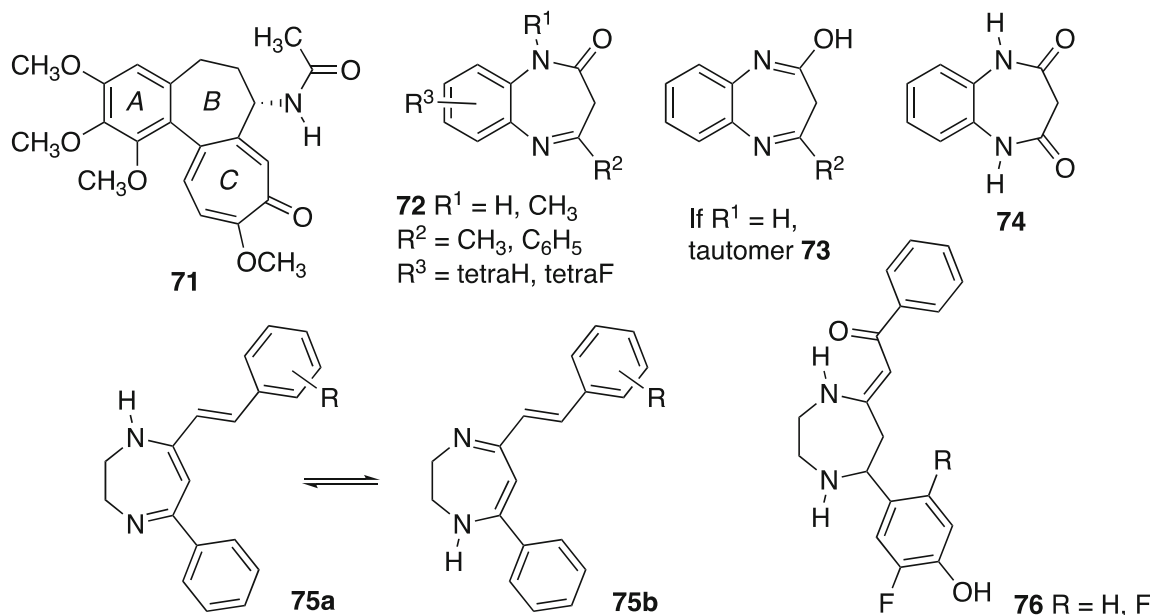
Another publication belonging to this section concerns the study of 1,3,5-triphenyl- Δ^2 -pyrazoline (or 4,5-dihydro-1*H*-pyrazole, **70**). Figure 9 shows that the X-ray structure (this

compound crystallizes as a conglomerate) and the optimized one (B3LYP/TZVP) are very similar [107]. Compound **70** has been proposed as organocatalyst via iminium activation [108].

Rings larger than six-membered

The minimum energy conformation of the seven-membered ring *B* of colchicine (**71**), a compound that continued to be much studied [109], has been calculated at the B3LYP/6-

311++G(d,p) level showing agreement with the X-ray structure and providing torsion angles consistent with vicinal ^1H – ^1H spin–spin coupling constants (Karplus equation) [110].



Seven-membered rings containing two nitrogen atoms are called diazepines, the most common are the benzo[*e*][1,4]-benzodiazepines, like chlordiazepoxide, diazepam, lorazepam, and many others. In our case, we have studied the benzo[*b*][1,4]benzodiazepines. In benzodiazepines **72** [111], **73** [111, 112], and **74** [113] and in diazepines **75a** and **b** [114] and **76** [115], tautomerism and ring inversion (none of these seven-membered rings are planar) have been computed at different levels.

A conformational analysis of 2,3,6,7-tetrahydroazepines was carried out with MM3 and CHARMM

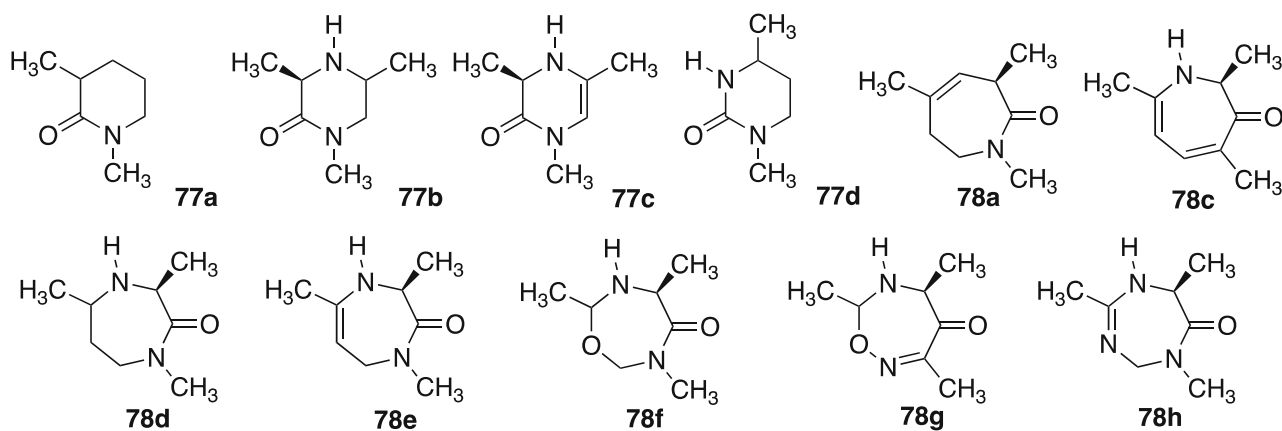
molecular mechanics, and AM1 semi-empirical, as well as Hartree–Fock and local density functional (LDF) ab initio methods [116]. Similar geometrical characteristics were found with all methods although there are important differences in the rank order of the relative energies. The importance of the solvation of these compounds in the affinity for the dopamine D1 receptor was also studied [117].



Fig. 12 A six-blade propeller

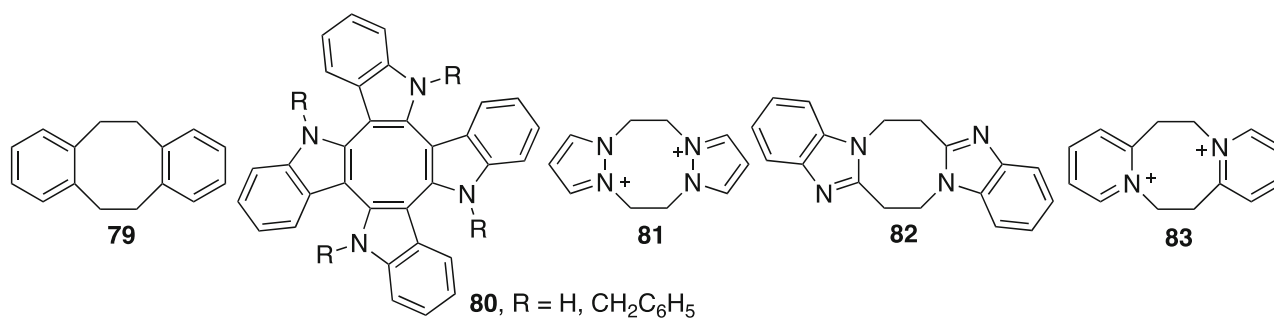


Fig. 13 A three-blade propeller



The ability of a series of six- **77** and seven-membered ring structures **78** to mimic the properties of an ideal γ -turn has been studied by means of three molecular similarity indices [118]. In general, the compounds with

seven-membered rings show good overall molecular similarity indices when compared to an ideal inverse γ -turn while six-membered rings provide good overall similarities with classic and inverse γ -turns.



5,6,11,12-Tetrahydrodibenzo[*a,e*]-cyclooctene or -[8]annulene (**79**) has three conformations: chair, twist-boat, and twist [119]; using GIAO/B3LYP/6-31G* calculations together with ¹H and ¹³C DNMR experiments, the long-standing problem of its conformation has been solved and the interconversion barriers determined. The two most stable conformations, chair and twist-boat, have similar energies and interconvert through processes having activation energies about 42 kJ mol⁻¹ slightly dependent on the solvent. The

different conformations have different sizes and that has been used to prepare a thermal contracting polymer [120, 121].

The tetraindoles **80** show ring inversion when R = H, inversion inhibited by *N*-substitution [122]. These multi-indole structures are part of the PAHs (polycyclic aromatic hydrocarbons) [123]. Conformational analysis of eight-membered rings containing four **81** or two N atoms, **82** and **83**, was carried out (B3LYP/6-311++G(d,p)) and compared with **75** [124]. The energy profiles are similar to those determined experimentally.

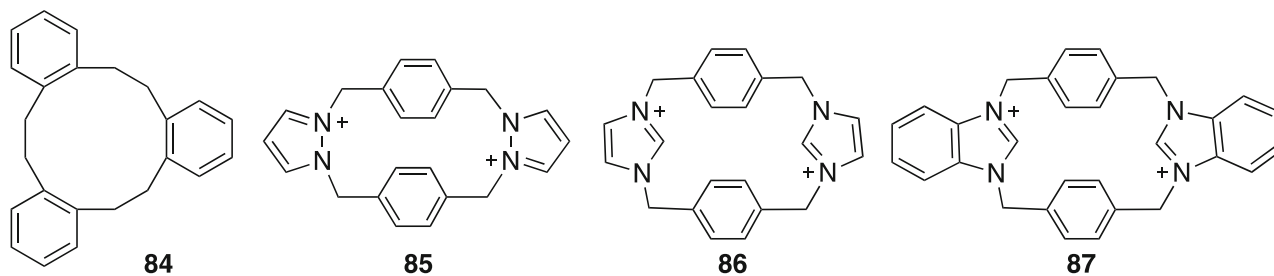


Table 1 Racemization barriers of helicenes in kilojoules per mole

Helicene	Experimental	Calculated	Our calculations ^a
[4] 125	–	18.8 [197]; 16.7 [198]	18.3
[5] 126	102.9 [192]	103.3 [197]; 102.1 [198]	102.0
[6] 127	151.5 [192]	157.3 [197]; 154.4 [198]	155.4
[7] 128	174.5 [192]	175.7 [198]	175.0
[8]	177.4 [192]	178.7 [198]	175.6
[9]	182.0 [192]	184.9 [198]	169.6
1-Methyl[6]	183.3 [199]		180.0
2-Methyl[6]	~ 151.5 [199]		156.2
1,16-Dimethyl[6]	184.1 [199]		181.0
2,15-Dimethyl[6]	162.3 [199]		163.5
2-Bromo[6]	152.7 [200]		148.8
2,15-Dibromo[6]	–		156.9
1,2,3,4-Tetrafluoro[6]	162.8 [193]		159.3
Dehydro[6]helicenes			
129a	71.1 [201]		66.7
129b	133.9 [201]		191.0
129c	136.4 [201]		211.9
129d	138.0 [201]		233.1
129e			136.7
129f			217.7

^a B3LYP/6-31G(d)

A few rings larger than 8-membered have been studied. The 12-membered ring derivative **84** has played an important role in the history of the conformational analysis. B3LYP/6-311++G(d,p) calculations allow to determine four minima and four TSs; the calculated ring inversion barrier, 42.6 kJ mol⁻¹, is in excellent agreement with the measured barrier 41.4 ± 0.8 kJ mol⁻¹ [125]. Sixteen-membered ring **85** and 18-membered rings **86** and **87** were studied (DNMR and crystallography) and their ring barriers measured and calculated with the AM1 Hamiltonian [126]. Compounds related to **86** and **87** but with *o*-phenyl groups instead of *p*-phenyl ones have been reported [127, 128].

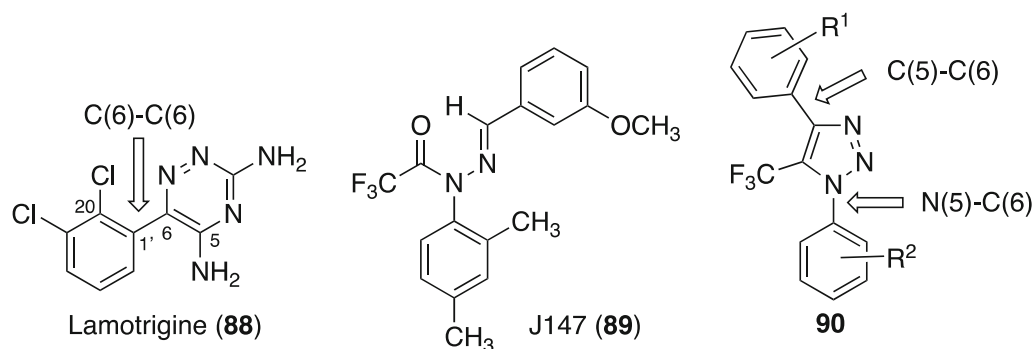
Chirality in molecules devoid of chiral centers

Biphenyls, atropisomerism

We have studied several of the ten possible situations of Fig. 10 in a paper covering many situations [129] and a

review reporting the literature until 2011 [130] (see also [131]). The nomenclature used in Fig. 10 to define each central bond includes the atoms involved in the bond and, between parentheses, the number of atoms in each ring.

Two papers were devoted to C(6)–C(6) systems, the first one to 1,1'-binaphthalenes bearing at positions 2,2' CH(OH)CF₃ substituents (three stereoisomers, *R,S,S*; *R,S,R*; and *R,R,R* and their enantiomers, combining axial and central chirality). B3LYP/6-31G(d) calculations were used to determine the mechanism of formation of the diols by reduction of the double COCF₃ derivatives [132]. The static and dynamic properties of BINOL (1,1'-bi-2-naphthol) and its conjugated acids and bases were studied using mass spectrometry, microwave rotational spectroscopy, NMR in superacid media, and MP2/6-311++G(d,p) calculations [133]. Our calculated BINOL barrier was used to discard a hypothetical mechanism [134].



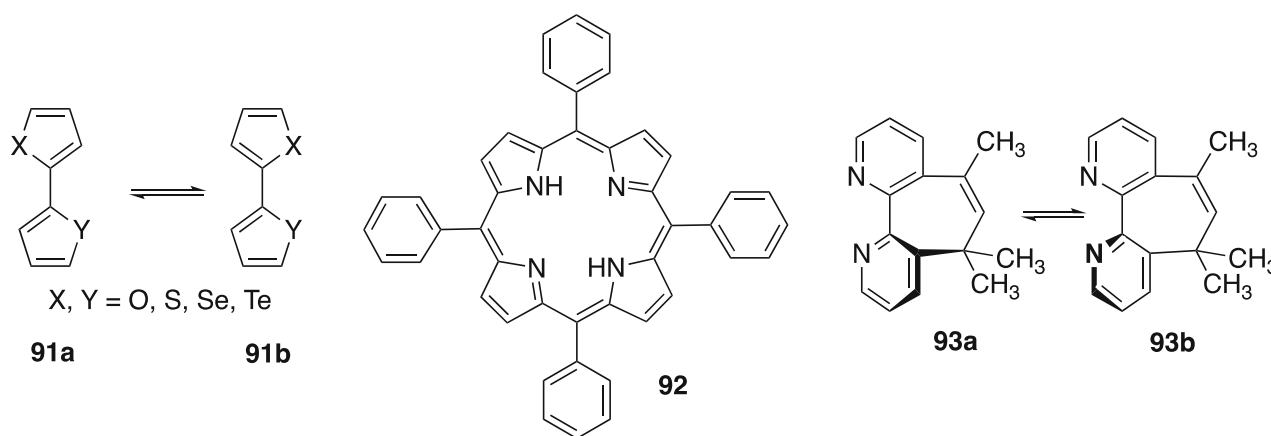
Lamotrigine (**88**), the treatment of choice for epilepsy and bipolar disorder, is a racemate of rapid interconverting enantiomers [135]; this was established by ^1H NMR at 600 MHz in the presence of ABTE (Virgili's [(*S,S*)- α,α' -bis(trifluoromethyl)-9,10-anthracenedimethanol] chiral auxiliary) and B3LYP/6-311++G(d,p) calculations. The predominance of the diamino structure proved relevant for the study of the hydrolysis of Lamotrigine-N2-glucuronide in wastewater [136].

We have calculated the barrier to the rotation about the C6–C1' bond through a near-planar structure that corresponds to a racemization process. There are two possibilities that correspond to diastereomers: that the Cl atom at position 20 is on the side of N1 (Fig. 11a) and that it is on the side of the 5-NH₂ (Fig. 11b). The barriers are almost the same, 61.9 and 62.1 kJ mol⁻¹,

respectively, therefore in the range that can be measured by dynamic NMR (DNMR) in the presence of a chiral additive. Using this technique, we have determined in CDCl₃ a value of $\Delta G_{\text{TC}}^\ddagger = 62.4$ kJ mol⁻¹, the agreement being excellent.

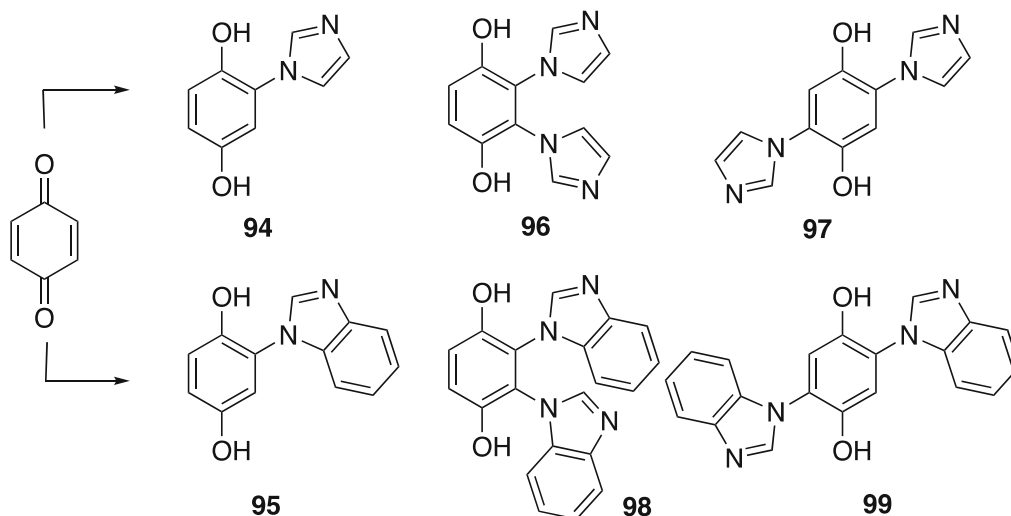
Compound J147 (**89**) is one of the most promising compounds to treat Alzheimer's disease [12] and it was used to design a series of 1,2,3-triazoles **90** whose conformational preferences were calculated [137].

Ten structures corresponding to two heterocycles C–C bonded, C(5)–C(5) **91**, were studied theoretically [MP2/6-311++G(d,p)] to see if chalcogen–chalcogen interactions (conformation **91b**) determined the preferred conformation. It appears that they are important although dipole–dipole effects also contribute [138].



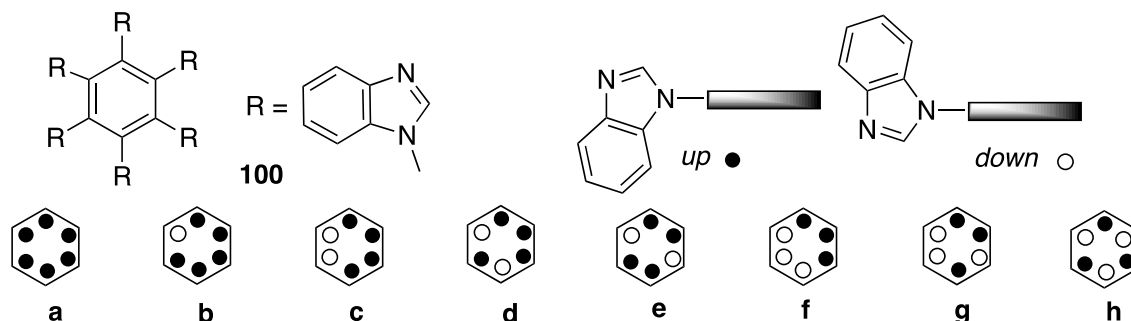
A review was published covering the conformational aspects of *meso*-tetraarylporphyrins (**92**) [139], not only with aryl but also with heteroaryl groups like pyridines and C-substituted pyrazoles yielding four atropisomers ($\alpha,\alpha,\beta,\beta$; $\alpha,\alpha,\alpha,\beta$; $\alpha,\beta,\alpha,\beta$; and $\alpha,\alpha,\alpha,\alpha$) that are conformationally stable at room temperature although they interconvert in solution

at high temperatures [140]. The conformation of 2,2', 3,3', and 4,4'-bipyridines as well as their monoprotonated and diprotonated forms was studied with particular emphasis on their NMR chemical shifts and conformational barriers [141] (see also [142]). The rates of enantiomerization of chiral 2,2'-bipyridines with restricted rotation **93a** and **b** were calculated [B3LYP/6-311++G(d,p)] [143].



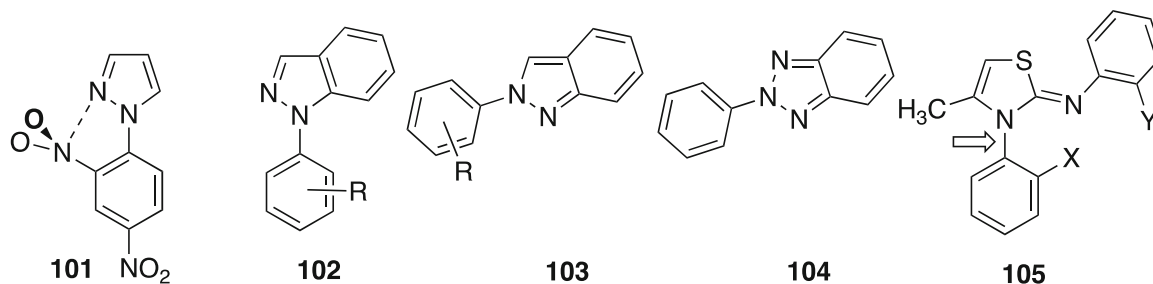
The most studied series in this section belong to Het(N)–Ar(C) compounds; only one was a six-membered heterocycle (a pyrimidin-2-thione) [144] cited by Roussel in [145], all the others were *N*-arylazoles N(5)–C(6). The addition of imidaz-

oles and benzimidazoles to quinones affords mono (**94**, **95**) and disubstituted derivatives (**96–99**) and related compounds; *meso* and *d,l* compounds are formed [146].



The reaction of hexafluorobenzene with sodium benzimidazolates affords hexakis (benzimidazol-1'-yl) benzenes **100** as the only products. These compounds, called propellenes [147] by analogy with hexaphenylbenzene

[148–150] (Fig. 12), present eight possible conformations depending on the up/down position of the benzimidazolyl residue; three of them have been characterized **c**, **f**, and **g** [151].



All of the above systems have been studied, each one presenting specific situations: **101** is an example of orthogonal interaction between the N atom of the nitro group and the N2 atom of the azole (besides pyrazoles, triazoles, tetrazoles, indazoles, and benzotriazoles have been studied) [152, 153]. *N*-Arylindazoles, both *1H* **102** and *2H* **103**, were examined starting from X-ray structures reported in the Cambridge Structural Database [154]; the search includes aza-derivatives (N atoms instead of CH groups in the six-membered ring) [155]. The 1,2,3-triazole **90** present also a conformation about an N–C bond

[137]. A series of 2-, 3-, 4-, 2,4- (like **101**), 2,6-, and 2,4,6-nitro-pyrazoles and indazoles were examined with special emphasis on the X-ray structures [156]. The chemical shifts of 2-phenyl-2*H*-benzotriazole (**104**) in the solid state were calculated with the GIPAW and GIAO-PCM (DMSO) and both methods compared; only for ¹⁵N SSNMR chemical shifts GIPAW proved better [157]. Finally, the atropisomerism of **105** was studied showing the influence of hydrogen bonding on the racemization rates that were determined by treatment of the plateau-shape chromatogram during chromatography on chiral

support [158] (for similar results, see [159]). An example of the much less frequent case where instead of an aryl ring there is a six-membered heterocycle concerns 2,4,6-tris(1*H*-pyrazol-1-yl)-1,3,5-triazine, a compound presenting polymorphism, pseudopolymorphism, and co-crystals [160].

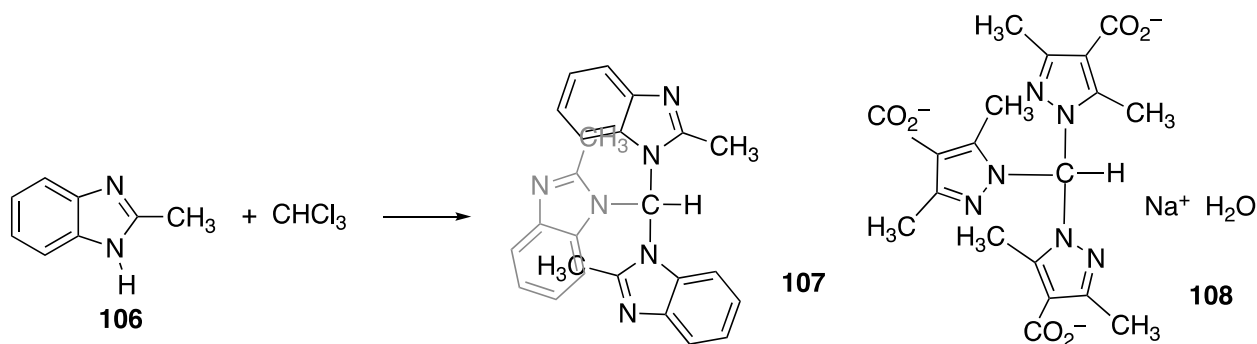
Molecular propellers

In this section, we will discuss three-blade propellers (Fig. 13) much more common than the previous six-blade ones [14, 161, 162]. Usually, they are tris-azolyl

derivatives related to trisarylmethanes [163–166]; the tetrakisazolyl derivatives, related to tetrakisarylmethanes [167–169], are less common.

Methanes

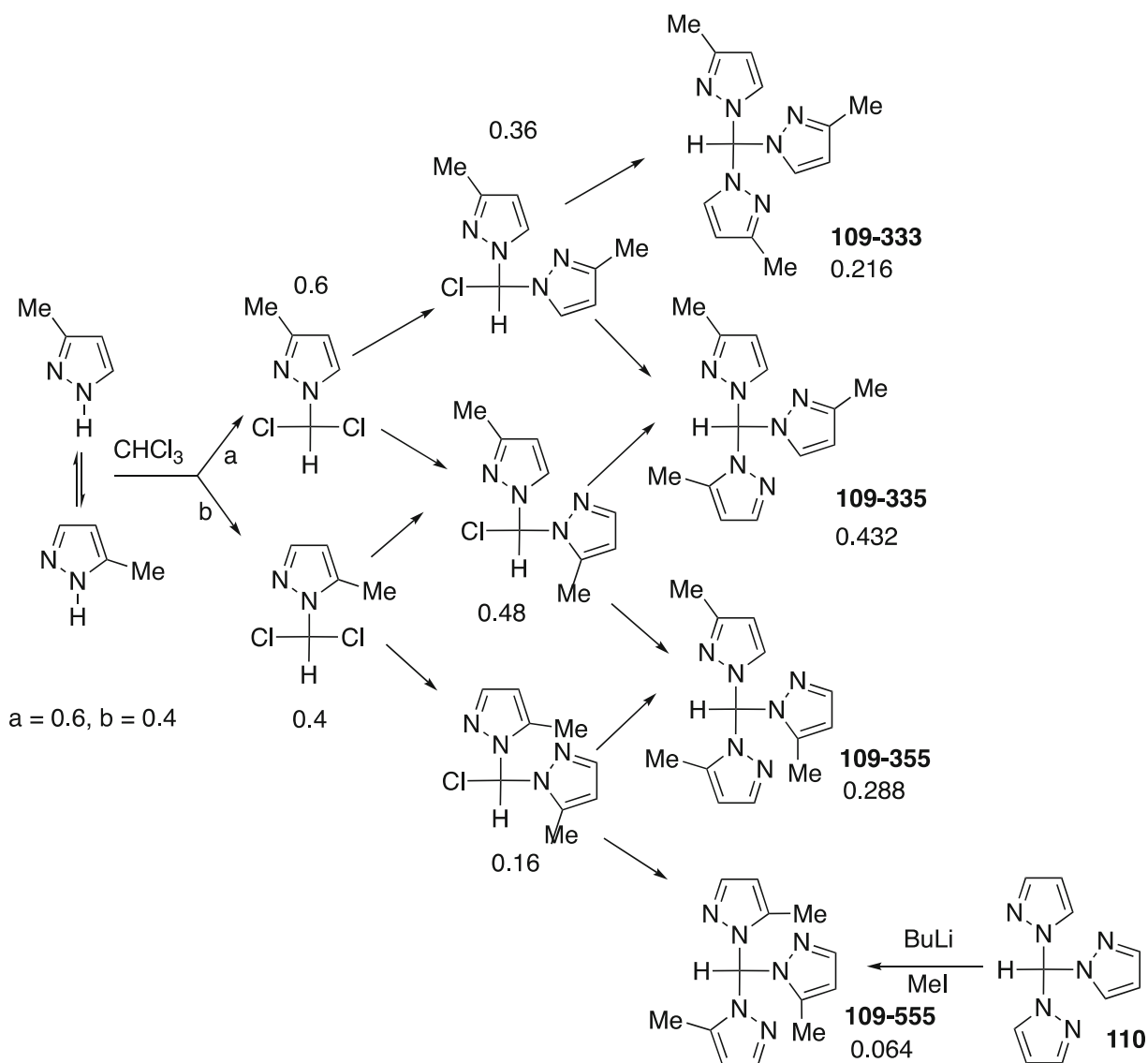
In 1994, Breitmaier et al. published a paper where Grignard alkylation of aldehydes occurs with very large enantiomeric excess due to the effect of the static magnetic field of an NMR spectrometer [170]. Since this result seems improbable, we carry out a reaction that we feel will be much more sensitive to chiral induction [164].



The reaction of 2-methyl-1*H*-benzimidazole (**106**) with chloroform in the conditions of PTC affords the tris(2-methylbenzimidazol-1-yl)methane (**107**) as a racemic that by ¹H NMR in the presence of Pirkle's alcohol was proved to be a 50:50 mixture of both enantiomers. The enantiomers were separated by chromatography on microcrystalline cellulose triacetate [171]; they are stable with a racemization barrier of 120 kJ mol⁻¹ at 343 K. When the reaction was carried out inside of an NMR spectrometer (7.05 T), we obtain again a 50:50 mixture, i.e., no enantioselectivity. We sent our paper to *Angewandte Chemie* where it was rejected based on "the journal does not published negative results." We sent it immediately to *Heterocyclic Communications* [172] where it was received on June 30, 1994.

Although *Heterocyclic Communications* continue to be published, the first issue where our paper appeared was not included in the Web of Science. Shortly afterwards, Breitmaier's paper was withdrawn [173–176]. A series of papers were published on this topic in subsequent years, by ours [177, 178] and by other groups [179, 180]. Among the derivatives studied, experimentally (X-ray) and theoretically, was **108** [181]. A comprehensive review on poly(pyrazol-1-yl)methanes up to 2017 was published [182].

The reaction of 3(5)-methyl-1*H*-pyrazole with CHCl₃ affords four tris(pyrazol-1-yl)methanes **109** in proportions that obey a (a + b)³ model (a = 3-methyl; b = 5-methyl) with great accuracy. Isomer **109-555** was prepared from tris pyrazol-1-yl)methane (**110**) [183].

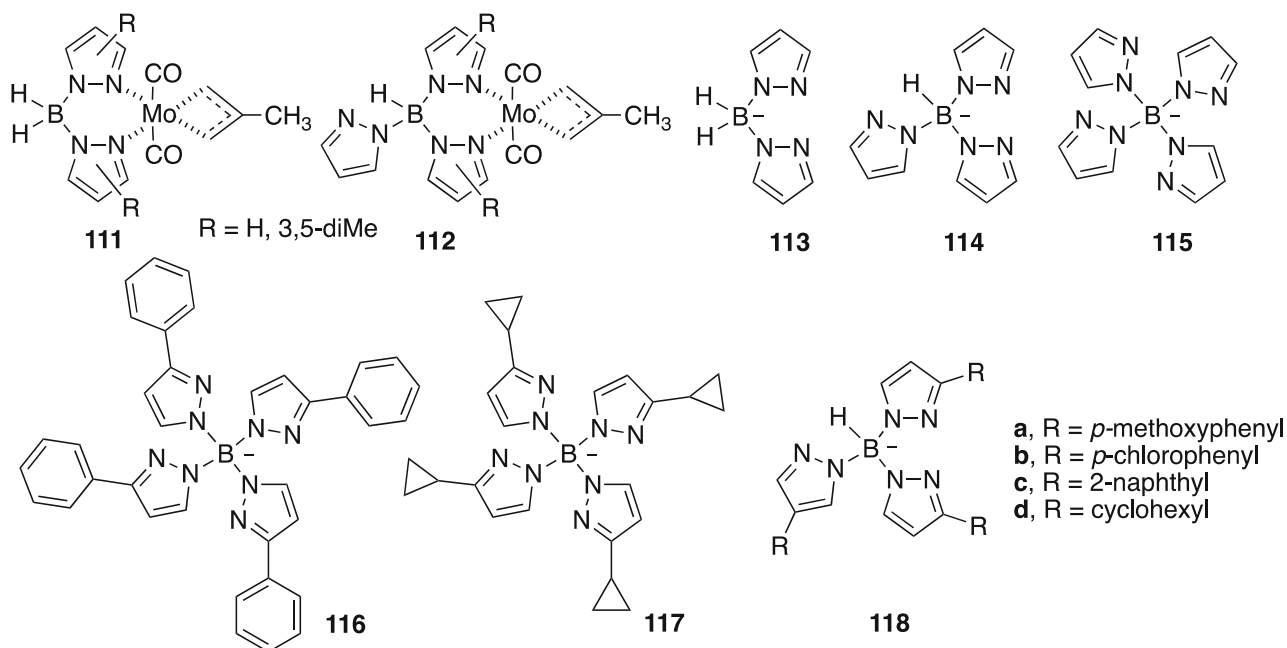


When the reaction was carried out with CCl_4 , the proportion of tetrakis derivatives does not follow an $(a + b)^4$ polynomial expansion, probably due to steric effects in the last step, going from Mepz_3Cl to Mepz_4C [184].

Borates (scorpionates)

Following Trofimenko's seminal work [185, 186] and sometimes collaborating with him [7, 187], we have

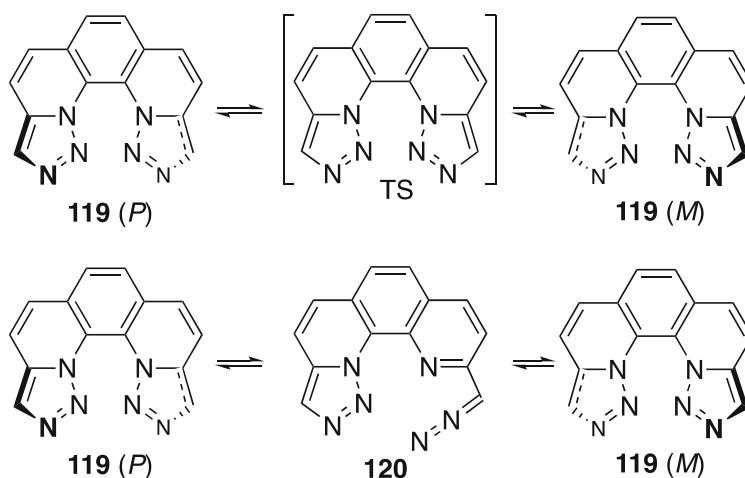
devoted some publications to the study of scorpionates mainly using NMR data and conformational analyses: fluxional behavior of **111** and **112** [188], multinuclear NMR and space groups **113–115** [189], crystallography and SSNMR of the thallium salts of scorpionates **116–117** with a discussion of the 11 motifs observed for tetrakis scorpionate derivatives [190], and the structure of four thallium tris(1*H*-pyrazol-1-yl)hydroborates **118a–118d** [191].



Helicenes

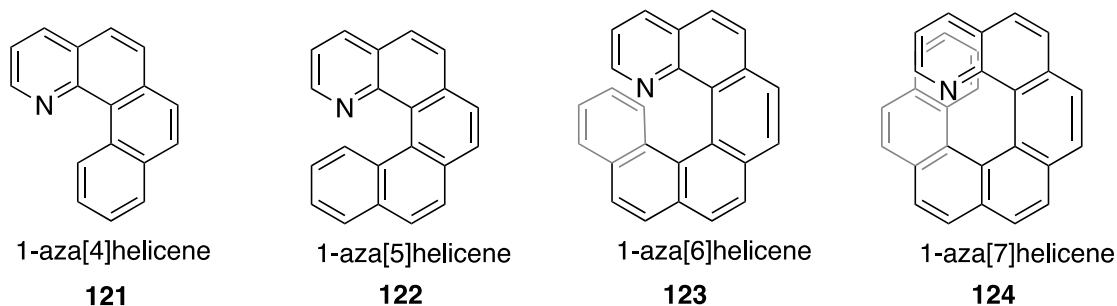
Helicenes are fascinating molecules [14, 162, 192] (for two recent publications related to our work, see [193, 194]) that we have studied three times. Hexaaza[5]helicenes **119** racemize

(*M/P* helix conversion) by a classical mechanism and not by a ring opening **120**/ring closing one [195]. The kinetic parameters are $\Delta H = 17.6 \text{ kJ mol}^{-1}$ and $\Delta S = 53.8 \text{ J mol}^{-1} \text{ K}^{-1}$.

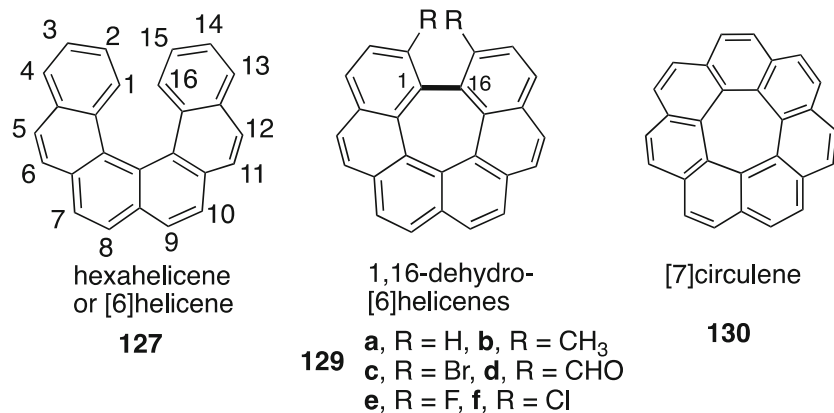
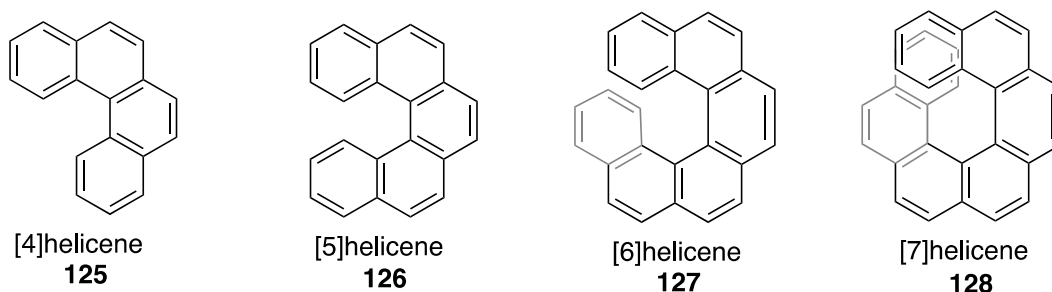


The racemization barriers of the 1-aza series **121–124** were calculated at the M05-2x/6-31G(d) level. The [4]helicene **121** is planar; for the three others, the barriers are 57.0 (**122**), 141.1 (**123**), and 181.6 kJ mol^{-1}

(**124**); the experimental value of **123** is 134.7 kJ mol^{-1} [196]. Dimers linked by alkaline cations (Li^+ , Na^+ , K^+) were calculated to study the chiral distinction between homochiral and heterochiral dimers.



We have in process the calculation of the barriers of helicenes reported in Table 1.



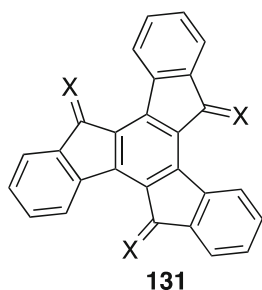
In the process of preparing [7]circulene (**130**), Yamamoto et al. went through 1,6-dehydro [6]helicenes **129a–129d** [201] determining the X-ray structure of **129c** and the racemization barriers of the four compounds (Table 1). Contrary to the barriers of helicenes that the calculations (different levels) reproduce with accuracy (Table 1), those of 1,6-dehydro[5]helicenes **129** (except **129a**, the less hindered) are grossly overestimated (increasing the level of the calculations, up to MP2 and CCSD does not solve the problem). A possible explanation is that the TS involves an open-shell diradicaloid structure.

The results of Table 1 shows that with a moderate level of calculation (M05-2x/6-31G(d)), the experimental results are well reproduced: Removing **129b** to **129d**, we obtain, Exp. = (1.012 ± 0.008) B3LYP/6-31G(d), $n = 12$, $R^2 = 0.999$. The deviation of compounds **129b** to **129d** can be calculated adding a dummy to be 78 ± 6 kJ mol⁻¹.

Truxenes

The only representative of this section are truxenes **131**, an interesting family of concave shape

hydrocarbons [202] that have been much studied by their proximity to fullerenes [123, 203, 204]. Truxene derivatives may be considered molecules with three helicene regions.



X = O, S, CH₂, CHF, CF₂, CCl₂

131

Conclusion

The great diversity of structures, **1–131**, added to the different techniques (solution and solid-state NMR, chiral reagents for enantioselective synthesis, dynamic NMR (DNMR) in the presence of a chiral additive, X-ray crystallography, circular dichroism, vibrational circular dichroism, chiral chromatography, kinetics, equilibria, etc.) were tied together by theoretical calculations. They provided a rationale for the measured values and, at the same time, allow predicting unmeasured properties.

The future of chemistry is tied to the progress in computational chemistry. The number of possible structures, being much larger than the elementary particles in the Universe [205] and the biased distribution of known molecules in the multidimensional space of chemical structures [206, 207], obliges to develop theoretical methods of prediction of properties (physical –materials– and biological –drugs–) to attain these compounds that will protect the humanity in the future.

This review reports many examples of the success of theoretical chemistry in explaining known properties; a step further is necessary to predict properties of unknown compounds. This should be the main conclusion of this review.

Acknowledgements We thank the reviewer for commentaries that led to an improvement of our manuscript.

Funding information This work was carried out with financial support from the Ministerio de Ciencia, Innovación y Universidades (Project PGC2018-094644-B-C2 2) and Dirección General de Investigación en Innovación de la Comunidad de Madrid (PS2018/EMT-4329 AIRTEC-CM). Thanks are also given to the CTI (CSIC) for their continued computational support.

Compliance with ethical standards

Conflict of interest The authors declare that they have no conflict of interest.

References

1. Elguero J, Silva AMS, Tomé AC (2011) Modern heterocyclic chemistry. In: Alvarez-Builla J, Vaquero JJ, Barluenga J (eds) Five-membered heterocycles: 1,2-Azoles, Part 1, Pyrazoles. Wiley-VCH, Weinheim
2. Foces-Foces C, Echevarría A, Jagerovic N, Alkorta I, Elguero J, Langer U, Klein O, Minguet-Bonvehí M, Limbach HH (2001) A solid-state NMR, X-ray diffraction, an *ab initio* computational study of hydrogen-bond structure and dynamics of pyrazole-4-carboxylic acid chains. *J Am Chem Soc* 123:7898–7906
3. Aguilar-Parrilla F, Cativiela C, De Villegas MDD, Elguero J, Foces-Foces C, Laureiro JIG, Cano FH, Limbach HH, Smith JAS, Toiron C (1992) The tautomerism of 3(5)-phenylpyrazoles: an experimental (¹H, ¹³C, ¹⁵N NMR and X-ray crystallography) study. *J Chem Soc Perkin Trans 2*:1737–1742
4. Alkorta I, Elguero J (2016) A computational study of azaphospholes: anions and neutral tautomers. *Struct Chem* 27: 1531–1542
5. Alkorta I, Sánchez-Sanz G, Elguero J (2012) Influence of hydrogen bonds on the P⋯P pnictogen bond. *J Chem Theor Comput* 8: 2320–2327
6. Brea O, Alkorta I, Mó O, Yáñez M, Elguero J, Corral I (2016) Exergonic and spontaneous production of radicals through beryllium bonds. *Angew Chem Int Ed* 55:8736–8739
7. López C, Claramunt RM, Trofimenko S, Elguero J (1993) A ¹³C NMR spectroscopy study of the structure of N-H pyrazoles and indazoles. *Can J Chem* 71:678–684
8. Alkorta I, Elguero J (2003) GIAO calculations of chemical shifts in heterocyclic compounds. *Struct Chem* 14:377–389
9. Del Bene JA, Perera SA, Bartlett RJ, Elguero J, Alkorta C, Alajarin M, Bautista D (2002) ³h/¹⁵N-³¹P Spin-spin coupling constants across N-H⋯O-P hydrogen bonds. *J Am Chem Soc* 124:6393–6397
10. Alkorta I, Elguero J, Del Bene JE, Mó O, Yáñez M (2010) New insights into factors influencing B-N bonding in X:BH_{3-n}F_n and X:BH_{3-n}Cl_n for X = N₂, HCN, LiCN, H₂CNH, NF₃, NH₃ and n = 0–3: the importance of deformation. *Chem Eur J* 16:11897–11905
11. Berthou J, Elguero J, Rérat R (1970) Raffinement de la structure cristalline du pyrazole. *Acta Crystallogr Sect B* 26:1880–1881
12. Clarkson GJ, Farrán MA, Claramunt RM, Alkorta I, Elguero J (2019) The structure of the anti-aging agent J147 used for treating Alzheimer's disease. *Acta Crystallogr Sect C* 75:271276
13. Alkorta I, Blanco F, Elguero J (2008) Proton transfer in C-halogen pyrazole cyclamers. A theoretical study (2008). *Struct Chem* 19: 181–198
14. Eliel EL, Wilen SH (with a contribution of LN Mander) (1994) Stereochemistry of organic compounds. John Wiley & Sons, New York
15. Alkorta I, Elguero J (1998) Dissociation energies and rotational barriers about CC single, double, and triple bonds: a hybrid HF-DFT approach (Becke3LYP/6-311++G**). *Struct Chem* 9:59–63
16. Wu LC, Hsu CW, Chuang YC, Lee GH, Tsai YC, Wang Y (2011) Bond characterization on a Cr-Cr quintuple bond: a combined experimental and theoretical study. *J Phys Chem A* 115: 12602–12615
17. Alkorta I, Wentrup C, Elguero J (2002) A theoretical study of the origin of rotational barriers in push-pull ethylenes. *J Mol Struct (THEOCHEM)* 585:27–34
18. Kostenko A, Tumanskii B, Karni M, Inoue S, Ichinoe M, Sekiguchi A, Apeloig Y (2015) Observation of a thermally accessible triplet state resulting from rotation around a main-group π bond. *Angew Chem Int Ed* 54:12144–12148
19. Feringa BL (2001) In control of motion: from molecular switches to molecular rotors. *Acc Chem Res* 34:504–513

20. Sánchez-Sanz G, Alkorta I, Elguero J (2011) Isomerization barriers in bis (4*H*-thiopyran) and in bithioxanthenes. *Tetrahedron* 67: 7316–7320
21. Langa F, de la Cruz P, Delgado JL, Haley MM, Shirtcliff L, Alkorta I, Elguero J (2004) The structure of *p*-nitrophenylhydrazones of aldehydes: the case of the *p*-nitrophenylhydrazone of 2-diethylamino-5-methoxy-2*H*-indazole-3-carboxaldehyde. *J Mol Struct* 699:17–21
22. Arnal E, Elguero J, Jacquier R, Marzin C, Wilde J (1965) Etude RMN d'azines. *Bull Soc Chim Fr* 877:878
23. Tabacik V, Pellegrin V, Elguero J, Jacquier R, Marzin C (1971) Symétrie et configuration de l'acétaldazine. Etude de spectres de vibration et de vibration-rotation. *J Mol Struct* 8:173–193
24. Elguero J, Jacquier R, Berthou J (1973) Etude comparative de la stéréochimie de quatre cinnamaldazines a l'état solide (rayons X) et en solution (UV, IR, RMN). *Bull Soc Chim Fr* 3303–3306
25. Safari J, Gandomi-Ravandi S (2014) Structure, synthesis and application of azines: a historical perspective. *RSC Adv* 4:46224–46249
26. Alkorta I, Blanco F, Elguero J (2008) Computational studies of the structure of aldazines and ketazines. Part 1. Simple compounds. *Arkivoc* vii:48–56
27. Blanco F, Alkorta I, Elguero J (2007) Computational studies of the structure of aldazines and ketazines. Part 2. Halogen and α,β -unsaturated derivatives. *J Mol Struct (THEOCHEM)* 847:25–31
28. Silva AMS, Silva VLM, Claramunt RM, Santa María D, Ferraro MB, Reviriego F, Alkorta I, Elguero J (2013) The structures of two aldazines: [1,1'-(1*E*,1'*E*)-hydrazine-1,2-diylidenebis(methan-1-yl-1-ylidene)dinaphthalen-2-ol] (Lumogen) and 2,2'-(1*E*,1'*E*)-hydrazine-1,2-diylidenebis(methan-1-yl-1-ylidene)diphenol (salicylaldazine) in the solid state and in solution. *Magn Reson Chem* 51:530–540
29. Pinto J, Silva VLM, Silva AMS, Claramunt RM, Sanz D, Torralba MC, Torres MR, Reviriego F, Alkorta I, Elguero J (2013) The structure of azines derived from C-formyl-1*H*-imidazoles in solution and in the solid state: tautomerism, configurational and conformational studies. *Magn Reson Chem* 51:203–221
30. Blanco F, Alkorta I, Elguero J (2009) Barriers about double carbon-nitrogen bond in imine derivatives (aldimines, oximes, hydrazones, azines). *Croat Chem Acta* 82:173–183
31. Gentili P, Nardi M, Antignano I, Cambise P, D'Abramo M, D'Acunzo F, Pinna A, Ussia E (2018) 2-(Hydroxyimino)aldehydes: photo- and physicochemical properties of a versatile functional group for monomer design. *Chem Eur J* 24:7683–7694
32. López-Tarifa P, Sánchez-Sanz G, Alkorta I, Elguero J, Sanz D, Perona A, Claramunt RM (2012) The tautomeric structures of 3(5),3'(5')-azopyrazole [(*E*)-1,2-di(1*H*-pyrazol-3(5)-yl)diazene]: The combined use of NMR and electronic spectroscopies with DFT calculations. *J Mol Struct* 1015:138–146
33. Alkorta I, Elguero J, Cintas P (2015) Adding only one priority rule allows extending CIP rules to supramolecular systems. *Chirality* 27:339–343
34. Elguero J (2016) Is it possible to extend the Cahn-Ingold-Prelog priority rules to supramolecular structures and coordination compounds using lone pairs? *Chem Int* 38:30–31
35. Alkorta I, Elguero J (2002) Molecular versus supramolecular chemistry: the rotational barriers about covalent bonds and hydrogen bonds. *Struct Chem* 13:97–98
36. Bouchet P, Elguero J, Jacquier R, Pereillo JM (1972) Etude par RMN de la configuration d'hydrazides. *Bull Soc Chim Fr* 2264–2272
37. Bouchet P, Coquelet C, Elguero J (1975) Vicinal interproton coupling through two heteroatoms. II. Coupling $^3J(\text{H-N-O-H})$ occurring in *N*-nitrophenylhydroxylamines. *Org Magn Reson* 7:247–248
38. Elguero J, Johnson BL, Pereillo JM, Pouzard G, Rajzmann M, Randall EW (1977) Constantes de couplage vicinales a travers deux heteroatomes. III. Calculs theoriques et mesures experimentales dans les hydrazines enrichies en ^{15}N . *Org Magn Reson* 9:145–147
39. Alkorta I, Elguero J (2004) Karplus-type relationships between scalar coupling constants: $^3J_{\text{HH}}$ molecular versus $^4J_{\text{HH}}$ supramolecular coupling constants. *Theor Chem Accounts* 111:31–35
40. Alkorta I, Elguero J (2003) The influence of chain elongation on Karplus-type relationships: a DFT study of scalar coupling constants in polyacetylene derivatives. *Org Biomol Chem* 1:585–587
41. Ambati J, Rankin SE (2010) Determination of ^{29}Si - ^1H spin-spin coupling constants in organoalkoxysilanes with nontrivial scalar coupling patterns. *J Phys Chem A* 114:12613–12621
42. Provasi FP, Aucar GA, Sauer SPA (2004) Large long-range F-F indirect spin-spin coupling constants. prediction of measurable F-F couplings over a few nanometers. *J Phys Chem A* 108: 5393–5398
43. Zborowski K, Alkorta I, Elguero J (2006) Effect of dimerization and racemization processes on the electron density and the optical rotatory power of hydrogen peroxide derivatives. *J Phys Chem A* 110:7247–7252
44. Alkorta I, Elguero J (2002) Discrimination of hydrogen-bonded complexes with axial chirality. *J Chem Phys* 117:6453–6568
45. Sánchez M, Ferraro MB, Alkorta I, Elguero J, Sauer SPA (2008) Atomic partition of the optical rotatory power of methylhydroperoxide. *J Chem Phys* 128:064318
46. Sánchez M, Alkorta I, Ferraro MB, Elguero J, Sauer SPA (2014) On the transferability of atomic contributions to the optical rotatory power of hydrogen peroxide, methyl hydroperoxide and dimethyl peroxide. *Mol Phys* 112:1624–1632
47. Alkorta I, Elguero J, Provasi PF, Ferraro MB (2011) Theoretical study of the 1:1 and 2:1 (homo- and heterochiral) complexes of XOOX' (X, X' = H, CH₃) with Lithium Cation. *J Phys Chem A* 115:7805–7810
48. Alkorta I, Elguero J, Provasi PF, Pagola GI, Ferraro MB (2011) Electric field effects on nuclear magnetic shielding on the 1:1 and 2:1 (homo- and heterochiral) complexes of XOOX' (X, X' = H, CH₃) with lithium cation and their chiral discrimination. *J Chem Phys* 135:104e116
49. Sánchez-Sanz G, Alkorta I, Elguero J (2011) Theoretical study of HXYH dimers (X, Y = O, S, Se). Hydrogen bonding and chalcogen-chalcogen interactions. *Mol Phys* 109:2543–2552
50. Azofra LM, Alkorta I, Elguero J (2014) Chiral discrimination in dimers of diphosphines PH₂-PH₂ and PH₂-PHF. *ChemPhysChem* 15:3663–3670
51. Alkorta I, Elguero J (2010) A theoretical study of the stationary structures of the methane surface with special emphasis on NMR properties. *Chem Phys Lett* 489:35–38
52. Jackowski K, Makulski W (2011) ^{13}C shielding scale for MAS NMR spectroscopy. *Magn Reson Chem* 49:600–602
53. Nieto CI, Cabildo P, García MA, Claramunt RM, Elguero J, Alkorta I (2018) Libration of phenyl groups detected by VT-SSNMR: comparison with X-ray crystallography. *Magn Reson Chem* 56:1083–1088
54. Quesada-Moreno MM, Cruz-Cabeza AJ, Avilés-Moreno JR, Cabildo P, Claramunt RM, Alkorta I, Elguero J, Zúñiga FJ, López-González JJ (2017) The curious case of 2-propyl-1*H*-benzimidazole in the solid state: an experimental and theoretical study. *J Phys Chem A* 121:5665–5674
55. Alkorta I, Elguero J (2019) The strange case of achiral compounds which were reported to always crystallize in the same chiral group. *Struct Chem* in press. <https://doi.org/10.1007/s11224-018-1276-0>
56. Pérez-Torralba M, Claramunt RM, Alkorta I, Elguero J (2007) Double addition of azoles to glyoxal: characterization of the bis-adducts and theoretical study of their structure. *Arkivoc* xii:55–66

57. García-Frutos EM, Gómez-Lor B, Monge A, Gutiérrez-Puebla E, Alkorta I, Elguero J (2008) Synthesis and preferred all-*syn* conformation of C_3 -symmetrical *N*-(Hetero)arylmethyl triindoles. *Chem Eur J* 14:8555–8561
58. García-Pérez D, López C, Claramunt RM, Alkorta I, Elguero J (2017) ^{19}F -NMR diastereotopic signals in two *N*- CHF_2 derivatives of (4*S*,7*R*)-7,8,8-trimethyl-4,5,6,7-tetrahydro-4,7-methano-2*H*-indazole. *Molecules* 22:2003
59. Sanz D, Claramunt RM, Roussel C, Alkorta I, Elguero J (2018) The structure of *N*-benzylazoles from pyrrole to carbazole: geometries and energies. *Indian J Heterocycl Chem* 28:1–9
60. Holzer W, Castoldi L, Kyselova V, Sanz D, Claramunt RM, Torralba MC, Alkorta I, Elguero J (2019) Multinuclear NMR spectra and GIAO/DFT calculations of *N*-benzylazoles and *N*-benzylbenzazoles. *Struct Chem* in press. <https://doi.org/10.1007/s11224-019-01310-3>
61. Alkorta I, Elguero J (2014) A theoretical study of the structure and protonation of Palbociclib (PD 0332991). *J Mol Struct* 1056–1057:209–215
62. Chen FQ, Liu CX, Zhang J, Xu WF, Zhang YJ (2018) Progress of CDK4/6 inhibitor Palbociclib in the treatment of cancer. *Anti Cancer Agents Med Chem* 18:1241–1251
63. Nieto CI, Cabildo P, Claramunt RM, Cornago P, Sanz D, Torralba MC, Torres MR, Ferraro MB, Alkorta I, Marín-Luna M, Elguero J (2016) The structure of β -diketones related to curcumin determined by X-ray crystallography, NMR (solution and solid state) and theoretical calculations. *Struct Chem* 27:705–730
64. Alkorta I, Elguero J (2011) Conformational analysis of *N,N'*-dinaphthyl heterocyclic carbenes: imidazol-2-ylidenes and imidazolin-2-ylidenes. *Struct Chem* 22:1087–1094
65. Risso V, Farran D, Javierre G, Naubron JV, Giorgi M, Piras P, Jean M, Vanthuyn N, Fruttero LD, Roussel C (2018) Atropisomerism in a 10-membered ring with multiple chirality axes: (3*Z*,9*Z*)-1,2,5,8-dithiadiazecine-6,7(5*H*,8*H*)-dione series. *J Organomet Chem* 83:7566–7573
66. Alkorta I, Elguero J (2004) A GIAO/DFT study of ^1H , ^{13}C and ^{15}N shieldings in amines and its relevance in conformational analysis. *Magn Reson Chem* 42:955–961
67. Alkorta I, Elguero J, Eric E (2004) Paradigms and paradoxes: the position of the lone pair in amines: a comparison between Bader's AIM approach and pure geometrical considerations. *Struct Chem* 15:599–604
68. Creve S, Nguyen MT (1998) Inversion processes in phosphines and their radical cations: when is a pseudo-Jahn-Teller effect operative. *J Phys Chem A* 102:6549–6557
69. Del Bene JE, Sánchez-Sanz G, Alkorta I, Elguero J (2012) Homo- and heterochiral dimers (PHFX)₂, X = Cl, CN, CH₃, NC: To what extent do they differ? *Chem Phys Lett* 538:14–18
70. Al-Otaibi JS, El Gogary TM, El-Demerdash SH (2018) Umbrella inversion and structure of phosphorus-containing compounds: a quantum chemical study. *J Theor Comput Chem* 17:1850042
71. Mó O, de Paz JLG, Yáñez M, Alkorta I, Elguero J, Goya P, Rozas I (1989) A molecular orbital study of the conformation (inversion and rotational barriers) and electronic properties of sulfamide. *Can J Chem* 67:2227–2236
72. Sanz D, Claramunt RM, Alkorta I, Sánchez-Sanz G, Elguero J (2012) The structure of Glibenclamide in the solid state. *Magn Reson Chem* 50:246–255
73. Alkorta I, Alvarado M, Elguero J, García-Granda S, Goya P, Jimeno ML, Menéndez-Taboada L (2009) The structure of Rimonabant in the solid state and in solution: an experimental and theoretical study. *Eur J Med Chem* 44:1864–1869
74. Hansen E, Lime E, Norrby PO, Wiest O (2016) Anomeric effects in sulfamides. *J Phys Chem A* 120:3677–3682
75. Yonashiro H, Higashi K, Morikawa C, Ueda K, Itoh T, Ito M, Masu H, Noguch S, Moribe K (2018) Morphological and physicochemical evaluation of two distinct Glibenclamide/hypromellose amorphous nanoparticles prepared by the antisolvent method. *Mol Pharm* 15:1587–1597
76. Scott CE, Ahn KH, Graf ST, Goddard WA, Kendall DA, Abrol R (2016) Computational prediction and biochemical analyses of new inverse agonists for the CB1 receptor. *J Chem Inf Model* 56:201–212
77. Marín-Luna M, Alkorta I, Elguero J (2015) Theoretical study of the geometrical, energetic and NMR properties of atranes. *J Organomet Chem* 794:206–215
78. Sánchez-Sanz G, Trujillo C, Alkorta I, Elguero J (2017) Modulation of in:out and out:out conformations in [X,X',X''] phosphatranes by Lewis acids. *Phys Chem Chem Phys* 19:20647–20656
79. Matthews AD, Gravalis GM, Schley ND, Johnson MW (2018) Synthesis, structure, and reactivity of palladium proazaphosphatane complexes invoked in C-N cross-coupling. *Organomet* 37:3073–3078
80. Lin YC, Gihula JC, Rodosevich AT (2018) Nontrigonal constraint enhances 1,2-addition reactivity of phosphazenes. *Chem Sci* 9:4338–4347
81. Azofra LM, Alkorta I, Elguero J, Popelier P (2012) Conformational study of the open-chain and furanose structures of D-erythrose and D-threose. *Carbohydr Res* 358:96–105
82. Azofra LM, Alkorta I, Elguero J (2013) Theoretical study of the mutarotation of erythrose and threose: acid catalysis. *Carbohydr Res* 372:1–8
83. Quesada-Moreno MM, Azofra LM, Avilés-Moreno JR, Alkorta I, Elguero J, López-González JJ (2013) Conformational preference and chiroptical response of carbohydrates of D-ribose and 2-deoxy-D-ribose in aqueous and solid phases. *J Phys Chem B* 117:14599–14614
84. Azofra LM, Quesada-Moreno MM, Alkorta I, Avilés-Moreno JR, López-González JJ, Elguero J (2014) Carbohydrates in the gas phase: conformational preference of D-ribose and 2-deoxy-D-ribose. *New J Chem* 38:529–538
85. Cardamone S, Popelier PLA (2015) Prediction of conformationally dependent atomic multipole moments in carbohydrates. *J Comput Chem* 36:2361–2373
86. Walczak DL, Nowacki A, Trzybinski D, Samaszko-Fiertek J, Mysszka H, Sikorski A, Liberek B (2017) Conformational studies of *N*-(α -D-glucopyranurono-6,3-lactone) and *N*-(methyl β -D-glucopyranuronate)-*p*-nitroanilines. *Carbohydr Res* 446:85–92
87. Wang WJ, Huang F, Sun CZ, Liu JB, Liu JB, Sheng XH, Chen DZ (2017) A theoretical insight into the formation mechanisms of C/N-ribonucleosides with pyrimidine and ribose. *Phys Chem Chem Phys* 19:10413–10426
88. Zeng Z, Bernstein ER (2017) Anionic fructose-related conformational and positional isomers assigned through PES experiments and DFT calculations. *Phys Chem Chem Phys* 19:23325–23344
89. Zeng Z, Bernstein ER (2017) Anionic ribose related species explored through PES experiments, DFT calculations, and through comparison with anionic fructose species. *Phys Chem Chem Phys* 19:28950–28962
90. Szczepaniak M, Moc J (2017) Anomerization reaction of bare and microhydrated D-erythrose via explicitly correlated coupled cluster approach. Two water molecules are optimal. *J Comput Chem* 38:288–303
91. Dudek M, Zajac G, Szafraniek E, Wiercigroch E, Tott S, Malek K, Kaczor A, Baranska M (2019) Raman optical activity and Raman spectroscopy of carbohydrates in solution. *Spectrochim Acta Part A* 206:597–612
92. McGill CJ, Westmoreland PR (2019) Monosaccharide isomer interconversions become significant at high temperatures. *J Phys Chem A* 123:120–131

93. Cavero E, Giménez R, Uriel S, Beltrán E, Serrano JL, Alkorta I, Elguero J (2008) The boat conformation in pyrazaboles. A theoretical and experimental study. *Cryst Growth Des* 8:838–847
94. Patil Y, Misra R (2017) Tetracyanobutadiene bridged ferrocene and triphenylamine functionalized pyrazabole dimers. *J Organomet Chem* 840:23–29
95. Jimeno ML, Benito MT, García Doyagüez E, Claramunt RM, Sanz D, Marín-Luna M, Alkorta I, Elguero J (2016) A theoretical and experimental NMR study of BODIPY 493/503: difluoro{2-[1-(3,5-dimethyl-2*H*-pyrrol-2-ylidene-*N*)ethyl]-3,5-dimethyl-1*H*-pyrrolato-*N*} boron. *Magn Reson Chem* 54:684–688
96. Alkorta I, Azofra LM, Sánchez-Sanz G, Elguero J (2012) A theoretical study of six-membered rings containing the –N=S–S=N–motif. *Struct Chem* 23:1245–1252
97. Alcamí M, Mó O, Yáñez M, Alkorta I, Elguero J (2002) Triaziridine and tetrazetidine vs. cyclic water trimer and tetramer: a computational approach to the relationship between molecular and supramolecular conformational analysis. *Phys Chem Chem Phys* 4:2123–2129
98. Peverati R, Siegel JS, Baldrige KK (2009) *Ab initio* quantum chemical computations of substituent effects on triaziridine strain energy and heat of formation. *Phys Chem Chem Phys* 11:2387–2395
99. Alkorta I, Cativiela C, Elguero J, Gil AM, Jiménez AI (2005) A theoretical study of the influence of nitrogen angular constraints on the properties of amides: rotation/inversion barriers and hydrogen bond accepting abilities of *N*-formylaziridine and -azirine. *New J Chem* 29:1450–1453
100. Szostak M, Aubé J (2013) Chemistry of bridged lactams and related heterocycles. *Chem Rev* 113:5701–5765
101. Chung BKW, White CJ, Scully CCG, Yudin AK (2016) The reactivity and conformational control of cyclic tetrapeptides derived from aziridine-containing amino acids. *Chem Sci* 7:6662–6668
102. Alkorta I, Elguero J, Zborowski K (2007) Chiral recognition in diaziridine clusters and the problem of racemization waves. *J Phys Chem A* 111:1096–1103
103. Lykke L, Halskov KS, Carlsen BD, Chen VX, Jørgensen KA (2013) Catalytic asymmetric diazirdination. *J Am Chem Soc* 135:4692–4695
104. Alkorta I, Picazo O, Elguero J (2006) Chiral recognition of self-complexes of tetrahydro-imidazo[4,5-*d*]imidazole derivatives: from dimers to heptamers. *J Phys Chem A* 110:2259–2268
105. Figuera N, Alkorta I, García-López MT, González-Muñiz R (1995) 2-Amino-3-oxohexahydro-indolizino[8,7-*b*]indole-5-carboxylate derivatives as new scaffolds for mimicking β -turn secondary structures. Molecular dynamics and stereoselective synthesis. *Tetrahedron* 51:7841–7856
106. García-López MT, Alkorta I, Domínguez MJ, González-Muñiz R, Herranz R, Johansen NL, Madsen K, Thøgersen H, Suzdak P (1995) Constrained C-terminal hexapeptide neurotensin analogues containing a 3-oxoindolizidine skeleton. *Lett Pept Sci* 1:269–276
107. Vanthuyne N, Roussel C, Naubron JV, Jagerovic N, Morales Lázaro P, Alkorta I, Elguero J (2011) Determination of the absolute configuration of 1,3,5-triphenyl-4,5-dihydropyrazole enantiomers by a combination of VCD, ECD measurements, and theoretical calculations. *Tetrahedron-Asymmetry* 22:1120–1124
108. Rodrigo E, Cid MB, Roussel C, Vanthuyne N, Reviriego F, Alkorta I, Elguero J (2016) A proof of concept: 2-pyrazolines (4,5-dihydro-1*H*-pyrazoles) can be used as organocatalysts *via* iminium activation. *Lett Org Chem* 13:414–419
109. Pierens GK, Venkatachalam TK, Reutens DC (2017) NMR and DFT investigations of structure of colchicine in various solvents including density functional calculations. *Sci Rep* 7:5605
110. Virgili A, Quesada-Moreno MM, Avilés-Moreno JR, López-González JJ, García MA, Claramunt RM, Torres MR, Jimeno ML, Reviriego F, Alkorta I, Elguero J (2014) A spectroscopic study of colchicine in the solid state and in solution by multinuclear magnetic resonance and vibrational circular dichroism. *Helv Chim Acta* 97:471–490
111. Pérez-Torralba M, Claramunt RM, García MA, López C, Torralba MC, Torres MR, Alkorta I, Elguero J (2013) Structure of 1,5-benzodiazepinones in the solid state and in solution: effect of the fluorination in the six-membered ring. *Beilstein J Org Chem* 9: 2158–2167
112. Martí O, Pérez-Torralba M, García MA, Claramunt RM, Torralba MC, Torres MR, Alkorta I, Elguero J (2016) Static and dynamic properties of fluorinated 4-aryl-1,5-benzodiazepinones. *Chem Select* 4:861–870
113. Claramunt RM, Alkorta I, Elguero J (2013) A theoretical study of the conformation and dynamic properties of 1,5-benzodiazepines and their derivatives. *Comput Theor Chem* 1019:108–115
114. Nieto CI, Andrade A, Sanz D, Claramunt RM, Torralba MC, Torres MR, Alkorta I, Elguero J (2017) Curcumin related 1,4-diazepines: Regioselective synthesis, structure analysis, tautomerism, NMR spectroscopy, X-ray crystallography, density functional theory and GIAO calculations. *Chem Select* 2:3732–3738
115. Nieto CI, Sanz D, Claramunt RM, Torralba MC, Torres MR, Alkorta I, Elguero J (2018) Molecular structure in the solid state by X-ray crystallography and SSNMR and in solution by NMR of two 1,4-diazepines. *J Mol Struct* 1155:205–214
116. Alkorta I, Villar HO, Cachau RE (1993) Conformational analysis of 2,3,6,7-tetrahydroazepines with implications for D1 selective benzazepines. *J Comput Chem* 14:571–578
117. Alkorta I, Villar HO, Pérez JJ (1993) Comparison of methods to estimate the free energy of solvation: importance in the modulation of the affinity of 3-benzazepines for the D1 receptor. *J Comput Chem* 14:620–626
118. Alkorta I, Suarez ML, Herranz R, González-Muniz R, García-López MT (1996) Similarity study on peptide γ -turn conformation mimetics. *J Mol Model* 2:16–25
119. Jimeno ML, Alkorta I, Elguero J, Anderson JE, Claramunt RM, Lavaldera JL (1998) Conformation of 5,6,11,12-tetrahydrodibenzo[*a,e*]cyclooctene: an experimental and theoretical NMR study. *New J Chem* 1079–1083
120. Shen X, Viney C, Johnson ER, Wang C, Lu JQ (2013) Large negative thermal expansion of a polymer driven by a submolecular conformational change. *Nat Chem* 5:1035–1041
121. Wang Z, Huang Y, Guo J, Li Z, Xu J, Lu JQ, Wang C (2018) Design and synthesis of thermal contracting polymer with unique eight-membered carbocycle unit. *Macromol* 51:1377–1385
122. Ruiz C, Monge A, Gutiérrez-Puebla E, Alkorta I, Elguero J, López Navarrete JT, Ruiz Delgado MC, Gómez-Lor B (2016) Saddle-shaped cyclic indole tetramers: 3D electroactive molecules. *Chem Eur J* 22:10651–10660
123. Li X, Wang C, Xue Y, Meng C, Lai WY, Huang W (2017) Unexpected one-pot synthesis of diindolotriazatruxene: a planar electron-rich scaffold toward highly π -extended PAHs. *Asian J Org Chem* 6:1749–1754
124. Alkorta I, Elguero J (2010) Conformational analysis of dibenzo[*a,e*]cyclooctadiene and three related heterocycles. *Struct Chem* 21: 885–891
125. Alkorta I, Elguero J (2016) Theoretical studies on the conformation of large carbocyclic rings. I. 5,6,11,12,17,18-hexahydrotribenzo[*a,e,i*]cyclododecane (1,2;5,6;9,10-tribenzododeca-1,5,8-triene). *Tetrahedron Lett* 57:1838–1842
126. Cabildo P, Sanz D, Claramunt RM, Boume SA, Alkorta I, Elguero J (1999) Synthesis and structural studies of some [1₄]paracyclobis-(1,2)pyrazolium- and (1,3)imidazolium-phanes. *Tetrahedron* 55:2327–2340
127. Alcalde E, Dinarès I, Mesquida N (2010) Imidazolium-based receptors. *Top Heterocycl Chem* 24:267–300

128. Wedlock LE, Barnard PJ, Filipovska A, Skelton BW, Berners-Price SJ, Baker MV (2016) Dinuclear Au(I) N-heterocyclic carbene complexes derived from unsymmetrical azolium cyclophane salts: potential probes for live cell imaging applications. *Dalton Trans* 45:12221–12236
129. Alkorta I, Elguero J (2011) A computational study of the conformation of heterocyclic systems related to biphenyl. *Comput Theor Chem* 964:25–31
130. Alkorta I, Elguero J, Roussel C, Vanthuyne N, Piras P (2012) Atropisomerism and axial chirality in heteroaromatic compounds. *Adv Heterocycl Chem* 105:1–188
131. Smyth JE, Butler NM, Keller PA (2015) A twist of nature – the significance of atropisomers in biological systems. *Nat Prod Rep* 32:1562–1583
132. Mendizabal J, de March P, Recasens J, Virgili A, Álvarez-Larena Á, Elguero J, Alkorta I (2012) New C₂-symmetry diols accumulating one stereogenic axis and two stereogenic centers. *Tetrahedron* 68:9645–9651
133. Alkorta I, Cancedda C, Cocinero EJ, Dávalos JZ, Écija P, Elguero J, González J, Lesarri A, Ramos R, Reviriego F, Roussel C, Uriarte I, Vanthuyne N (2014) Static and dynamic properties of 1,1'-bi-2-naphthol and its conjugated acids and bases. *Chem Eur J* 20:14816–14825
134. Octa-Smolín F, van der Vight F, Yadav R, Bhangu J, Soloviova K, Wölper C, Daniliuc CG, Strassert CA, Somnitz H, Jansen G, Niemeyer J (2018) Synthesis of furan-annelated BINOL derivatives: acid-catalyzed cyclization induces partial racemization. *J Organomet Chem* 83:14568–14587
135. Alkorta I, Elguero J, Font A, Gálcera J, Mata I, Molins E, Virgili A (2014) An experimental and theoretical study of Lamotrigine in its neutral and protonated forms: evidence of Lamotrigine enantiomers. *Tetrahedron* 70:2784–2795
136. Zonja B, Delgado A, Abad JL, Pérez S, Barceló D (2016) Abiotic amidine and guanidine hydrolysis of lamotrigine-N2-glucuronide and related compounds in wastewater: the role of pH and N2-substitution on reaction kinetics. *Water Res* 100:466–475
137. Farrán MA, Bonet MA, Claramunt RM, Torralba MC, Alkorta I, Elguero J (2018) The structures of 1,4-diaryl-5-trifluoromethyl-1H-1,2,3-triazoles related to J147, a drug for treating Alzheimer's disease. *Acta Crystallogr Sect C* 74:513–522
138. Sánchez-Sanz G, Alkorta I, Elguero J (2011) A theoretical study of the conformation of 2,2'-bifuran, 2,2'-bithiophene, 2,2'-bitelluraphene and mixed derivatives: chalcogen–chalcogen interactions or dipole–dipole effects? *Comput Theor Chem* 974:37–42
139. Tomé AC, Silva AMS, Alkorta I, Elguero J (2011) Atropisomerism and conformational aspects of meso-tetrarylporphyrins and related compounds. *J Porphyrins Phthalocyanins* 15:1–28
140. Zardi P, Roisnel T, Gramage-Doria R (2019) A supramolecular palladium catalyst displaying substrate selectivity by remote control. *Chem Eur J* 25:627–634
141. Alkorta I, Elguero J, Roussel C (2011) A theoretical study of the conformation, basicity and NMR properties of 2,2'-, 3,3'- and 4,4'-bipyridines and their conjugated acids. *Comput Theor Chem* 966:334–339
142. Schneider HJ (2016) Efficiency parameters in artificial allosteric systems. *Org Biomol Chem* 14:7994–8001
143. Alkorta I, Elguero J, Roussel C (2011) Rates of enantiomerization of axially chiral 2,2'-bipyridines with restricted rotation: an *ab initio* study. *Tetrahedron-Asymmetry* 22:1180–1183
144. Najahi E, Vanthuyne N, Nepveu F, Jean M, Alkorta I, Elguero J, Roussel C (2013) Atropisomerization in *N*-aryl-2(1*H*)-pyrimidin-(thi)ones: a ring-opening/rotation/ring-closure process in place of a classical rotation around the pivot bond. *J Organomet Chem* 78:12577–12584
145. Belot V, Farran D, Jean M, Albalat M, Vanthuyne N, Roussel C (2017) Steric scale of common substituents from rotational barriers of *N*-(*o*-substituted aryl)thiazoline-2-thione atropisomers. *J Organomet Chem* 82:10188–10200
146. Escolástico C, Santa María MD, Claramunt RM, Jimeno ML, Alkorta I, Foces-Foces C, Hernández Cano F, Elguero J (1994) Imidazole and benzimidazole addition to quinones. Formation of *meso* and *d,l* isomers and crystal structure of the *d,l* isomer of 2,3-bis(benzimidazol-1-yl)-1,4-dihydroxybenzene. *Tetrahedron* 43:12489–12510
147. Claramunt RM, Elguero J, Escolástico C, Fernández-Castaño C, Foces-Foces C, Llamas-Saiz AL, Santa María MD (1997) Polyazolybenzenes and related compounds: propellene-like aromatic molecules, targets in heterocyclic systems, vol 1. Italian Society of Chemistry, Roma, pp 1–56
148. Almendinger A, Bastiansen O, Skancke PN (1958) Electron diffraction studies of hexaphenylbenzene vapour. *Acta Chem Scand* 12:1215–1220
149. Kosaka T, Inoue Y, Mori T (2016) Toroidal interaction and propeller chirality of hexaarylbenzenes. Dynamic domino inversion revealed by combined experimental and theoretical circular dichroism studies. *J Phys Chem Lett* 7:783–788
150. Yang Y, Chang Z, Yang X, Qi M, Wang J (2018) Selectivity of hexaphenylbenzene-based hydrocarbon stationary phase with propeller-like conformation for aromatic and aliphatic isomers. *Anal Chim Acta* 1016:69–77
151. Cornago P, Claramunt RM, Santa María MD, Alkorta I, Elguero J (1998) Aromatic propellenes. Part 9. Synthesis and conformational study of hexakis(benzimidazol-1'-yl)benzenes. *Model Chem* 135:475–483
152. Yap GPA, Jové FA, Claramunt RM, Sanz D, Alkorta I, Elguero J (2005) The X-ray molecular structure of 1-(2',4'-dinitrophenyl)-1,2,3-triazole and the problem of the orthogonal interaction between a “pyridine-like” nitrogen and a nitro group. *Aust J Chem* 58:817–822
153. Paulini R, Müller K, Diederich F (2005) Orthogonal multipolar interactions in structural chemistry. *Angew Chem Int Ed* 44:1788–1805
154. Allen FH (2002) The Cambridge Structural Database: a quarter of a million crystal structures and rising. *Acta Crystallogr Sect B* 58:380–388
155. Alkorta I, Elguero J (2017) The structure of *N*-arylidazoles and their aza-derivatives in the solid state: a systematic analysis of the Cambridge Structural Database coupled with DFT calculations. *J Mol Struct* 1137:186–192
156. Claramunt RM, Santa María D, Alkorta I, Elguero J (2018) The structure of *N*-phenyl pyrazoles and indazoles: Mononitro, dinitro, and trinitro derivatives. *J Heterocyclic Chem* 55:44–64
157. Marín-Luna M, Alkorta I, Elguero J (2018) A theoretical NMR study of selected benzazoles: comparison of GIPAW and GIAO-PCM (DMSO) calculations. *Magn Reson Chem* 56:164–171
158. Roussel C, Vanthuyne N, Boučekara M, Djafri A, Elguero J, Alkorta I (2008) Atropisomerism in the 2-arylimino-*N*-(2-hydroxyphenyl)thiazoline series: influence of hydrogen bonding on the racemization process. *J Organomet Chem* 73:403–411
159. Wu Y, Wang G, Li Q, Xiang J, Jiang H, Wang Y (2018) A multistage rotational speed changing molecular rotor regulated by pH and metal cations. *Nat Commun* 9:1953
160. Alkorta I, Reviriego F, Elguero J, Monge MA, Gutiérrez-Puebla E (2018) The structure of 2,4,6-tris(1*H*-pyrazol-1-yl)-1,3,5-triazine in the solid state: on polymorphs, pseudo-polymorphs and co-crystals. *Struct Chem* 29:15–21
161. Bürgi HB, Dunitz JD (1994) *Structure Correlation*. Volume 1. VCH, Weinheim

162. Wolf C (2008) Dynamic stereochemistry of chiral compounds. Principles and applications. The Royal Society of Chemistry, Thomas Graham House, Cambridge
163. Mislow K (1976) Stereochemical consequences of correlated rotation in molecular propellers. *Acc Chem Res* 9:26–33
164. Foces-Foces C, Hernández Cano F, Martínez-Ripoll M, Faure R, Roussel C, Claramunt RM, López C, Sanz D, Elguero J (1990) Complete energy profile of a chiral propeller compound: tris-(2'-methyl-benzimidazol-1-yl)methane (TMBM). Chromatographic resolution on triacetyl cellulose, X-ray structures of the racemic and one enantiomer, and dynamic NMR study. *Tetrahedron-Asymmetry* 1:65–86
165. Sedó J, Ventosa N, Molins MA, Pons M, Rovira C, Veciana J (2001) Stereoisomerism of molecular multipropellers. 2. Dynamic stereochemistry of bis- and tris-triaryl systems. *J Organomet Chem* 66:1579–1589
166. Ratera I, Veciana J (2012) Playing with organic radicals as building blocks for functional molecular materials. *Chem Soc Rev* 41:303–349
167. Claramunt RM, Elguero J, Fabre MJ, Foces-Foces C, Hernández Cano F, Hernández Fuentes I, Jaime C, López C (1989) A conformational study of bis-, tris- and tetrakis-pyrazolylmethane. Crystallography, L.S.R. dipole moments and theoretical calculations. *Tetrahedron* 45:7805–7816
168. Zimmermann TJ, Freundel O, Gompper R, Müller TJJ (2000) Synthesis and electronic properties of tetrakis[4-(pyrimidyl)phenyl]methanes – a novel class of electronically active nanometer-sized scaffolds. *Eur J Org Chem* 3305–3312
169. Zareba JK, Bialek MJ, Janczak J, Zón J, Dobosz A (2014) Extending the family of tetrahedral tectons: phenyl embraces in supramolecular polymers of tetraphenylmethane-based tetraphosphonic acid templated by organic bases. *Cryst Growth Des* 14:6143–6153
170. Zadel G, Eisenbraun C, Wolff GJ, Breitmaier E (1994) Enantioselective reactions in a static magnetic field. *Angew Chem Int Ed* 33:454–456
171. Bobosik V, López C, Claramunt RM, Roussel C, Stein JL, Thiery D, Elguero J (1993) Synthesis and resolution of bis- and tris-(benzimidazol-1-yl)methanes. *Heterocycles* 35:1067–1074
172. Elguero J, Jagerovic N, Werner A, Jimeno ML (1994) Failed attempt to induce chirality using a magnetic field: the case of chiral helicity of tris(2-methylbenzimidazol-1-yl)methane. *Heterocycl Commun* 1:101–102
173. Göllitz P (1994) Enantioselective reactions in a static magnetic field A false alarm! *Angew Chem Int Ed* 33:1457
174. Feringa BL, Kellogg RM, Hulst R, Zondervan C, Kruizinga WH (1994) Attempts to carry out enantioselective reactions in a static magnetic field. *Angew Chem Int Ed* 33:1458–1459
175. Kaupp G, Marquardt T (1994) Absolute asymmetric synthesis solely under the influence of a static homogeneous magnetic field? *Angew Chem Int Ed* 33:1459–1461
176. Breitmaier E (1994) No enantioselective reactions in a static magnetic field. *Angew Chem Int Ed* 33:1207
177. Alkorta I, Elguero J (2010) A theoretical analysis of the conformational space of tris(2-methylbenzimidazol-1-yl)methane. *Tetrahedron-Asymmetry* 21:437–442
178. Alkorta I, Elguero J (2009) Chirality and chiral recognition, Chapter 3. In: Leszczynski J, Shukla MK (eds) *Practical Aspects of Computational Chemistry. Methods, concepts and applications*. Springer, Heidelberg, pp 37–86
179. Avalos M, Babiano R, Cintas P, Jiménez JL, Palacios JC, Barron LD (1998) Absolute asymmetric synthesis under physical fields: facts and fiction. *Chem Rev* 98:2391–2404
180. Pagola GI, Ferraro MB, Provasi PF, Pelloni S, Lazeretti P (2019) Could electronic apolar interactions drive enantioselective syntheses in strongly nonuniform magnetic fields? A computational study. *J Chem Theor Comput* 15:961–971
181. Alkorta I, Elguero J, García MA, López C, Claramunt RM, Andrade GA, Yap GPA (2013) A tris(pyrazol-1-yl)methane bearing carboxylic acid groups at position 4: {1-[bis(4-carboxy-3,5-dimethyl-1H-pyrazol-1-yl)methyl]-3,5-dimethyl-1H-pyrazole-4-carboxylato}. *Acta Crystallogr Sect C* 69:972–976
182. Alkorta I, Claramunt RM, Díez-Barra E, Elguero J, de la Hoz A, López C (2017) The organic chemistry of poly(1H-pyrazol-1-yl)methanes. *Coord Chem Rev* 339:153–182
183. Silva VLM, Silva AMS, Claramunt RM, Sanz D, Infantes L, Martínez López A, Reviriego F, Alkorta I, Elguero J (2019) An example of polynomial expansion: the reaction of 3(5)-methyl-1H-pyrazole with chloroform and characterization of the four isomers. *Molecules* 24:568
184. Silva VLM, Silva AMS, Claramunt RM, Nieto CI, López C, Sanz D, Infantes L, Martínez López A, Reviriego F, Alkorta I, Elguero J (2019) New tetrakis(1H-pyrazol-1-yl)methanes. Manuscript in preparation
185. Trofimenko S (1966) Boron-pyrazole chemistry. *J Am Chem Soc* 88:1842–1844
186. Trofimenko S (1999) Scorpionates: polypyrazolylborate ligands and their coordination chemistry. Imperial College Press, London
187. Trofimenko S, Yap GPA, Jové FA, Claramunt RM, García MA, Santa María MD, Alkorta I, Elguero J (2007) Structure and tautomerism of 4-bromo substituted 1H-pyrazoles. *Tetrahedron* 63:8104–8111
188. Santa María MD, Claramunt RM, Alkorta I, Elguero J (2007) A theoretical and experimental study of the fluxional behaviour of molybdenum dihydrobis- and hydrotris-pyrazolylborates. *Dalton Trans* 3995–3999
189. Alkorta I, Elguero J, Claramunt RM, López C, Sanz D (2010) A theoretical multinuclear NMR study of pyrazolylborates. *Heterocycl Commun* 16:261–268
190. Infantes L, Claramunt RM, Sanz D, Alkorta I, Elguero J (2016) The structures of two scorpionates: thallium tetrakis(3-phenyl-1H-pyrazol-1-yl)borate and potassium tetrakis(3-cyclopropyl-1H-pyrazol-1-yl)borate. *Acta Crystallogr Sect C* 72:819–825
191. Infantes L, Moreno JM, Claramunt RM, Sanz D, Alkorta I, Elguero J (2018) The structure of four thallium tris(1H-pyrazol-1-yl)hydroborates in the solid state by X-ray crystallography and in solution by NMR and DFT-GIAO calculations. *Inorg Chim Acta* 483:402–410
192. Chen CF, Shen Y (2017) Helicene chemistry: from synthesis to applications. Springer-Verlag, Berlin
193. Církva V, Jakubík P, Strasak T, Hrbáč J, Sykora J, Cisarová I, Vacek J, Zádny J, Storch J (2019) Preparation and physicochemical properties of [6]helicenes fluorinated at terminal rings. *J Organomet Chem* 84:1980–1993
194. Salerno F, Rice B, Schmidt JA, Fuchter MJ, Nelson J, Jelfs KE (2019) The influence of nitrogen position on charge carrier mobility in enantiopure aza[6]helicene crystals. *Phys Chem Chem Phys* 21:5059–5067
195. Abarca B, Ballesteros R, Adam R, Ballesteros-Garrido R, Leroux FR, Colobert F, Alkorta I, Elguero J (2014) A theoretical and experimental study of the racemization process of hexaaza[5]helicenes. *Tetrahedron* 70:8750–8757
196. Alkorta I, Blanco F, Elguero J, Schröder D (2010) Distinction between homochiral and heterochiral dimers of 1-aza[n]helicenes ($n = 1-7$) with alkaline cations. *Tetrahedron-Asymmetry* 21:962–968
197. Goerick L, Sharma R (2016) The INV24 test set: How well do quantum-chemical methods describe inversion and racemization barrier? *Can J Chem* 94:1133–1143

198. Barroso J, Cabellos JL, Pan S, Murillo F, Zarate X, Fernández-Herrera MA, Merino G (2018) Revisiting the racemization mechanism of helicenes. *Chem Commun* 54:188–191
199. Janke RH, Haufe G, Würthwein EU, Borkent JH (1996) Racemization barriers of helicenes: a computational study. *J Am Chem Soc* 118:6031–6035
200. Jakubec M, Beránek T, Jakubíc P, Sykora J, Zádny J, Církva V, Storch J (2018) 2-Bromo[6]helicene as a key intermediate for [6]helicene functionalization. *J Organomet Chem* 83:3607–3616
201. Yamamoto K, Harada T, Okamoto Y, Chikamatsu H, Nakazaki M, Kai Y, Nakao T, Tanaka M, Harada S, Kasai N (1988) Synthesis and molecular structure of [7]circulene. *J Am Chem Soc* 110:3578–3584
202. Alkorta I, Blanco F, Elgyero J (2008) Theoretical study of racemization in chiral alkenylidene truxenes. *J Phys Org Chem* 21:381–386
203. Pérez EM, Illescas BM, Herranz MA, Martín N (2009) Supramolecular chemistry of π -extended analogues of TTF and carbon nanostructures. *New J Chem* 33:228–234
204. Goubard F, Dumur F (2015) Truxene: a promising scaffold for future materials. *RSC Adv* 5:3521–3551
205. Elguero J (2017) Hombres de ciencia y creadores: eso somos los químicos. *An Quim* 113:218–233
206. Reymond JL (2015) The chemical space project. *Acc Chem Res* 48:722–730
207. Delalande C, Awale M, Rubin M, Probst D, Ozthathil LC, Gertsch J, Abriel H, Reymond JL (2019) Optimizing TRPM4 inhibitors in the MHFP6 chemical space. *Eur J Med Chem* 166:167–177

Publisher's note Springer Nature remains neutral with regard to jurisdictional claims in published maps and institutional affiliations.